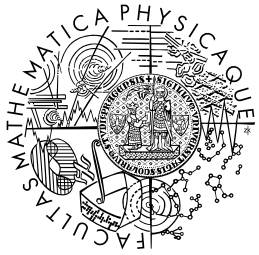

FACULTY
OF MATHEMATICS
AND PHYSICS
Charles University

HABILITATION THESIS

Vojtěch Patkóš

Precision calculations of light atomic spectra

Department of chemical physics and optics

Prague 2024

I would like to express my deepest gratitude to all my teachers and colleagues who helped me deepen my knowledge of physics. Most importantly, I want to thank my thesis supervisor Jaroslav Zamastil, my postdoc supervisor Krzysztof Pachucki, and my co-author Vladimir Yerokhin, who not only were my colleagues but also became my friends. I also thank my family for their continuous support, without which I would not have been able to accomplish this work.

Contents

Notations and conventions

Throughout the thesis we work in relativistic units $\hbar = c = 1$. In relativistic units the relation between the charge of the electron e and the fine structure constant is $e^2/4\pi = \alpha$. Energy levels and transitions between them are presented in Hz or in eV.

γ^μ	Dirac gamma matrices
$\vec{\alpha}$, β	Dirac matrices
σ^i	Pauli matrices
α	fine structure constant
$g^{\mu\nu}$	metric tensor
eA_μ	electromagnetic four-potential
$\Pi_\mu = p_\mu - eA_\mu$	physical four-momentum
$\hat{H}$	Hamilton operator
ψ	wave function
E	energy
E_F	Fermi splitting
$\vec{r}_a$	position of electron a
$\vec{r}_{ab}$	relative position of electrons a and b
g	g-factor of particle
κ_e	anomalous magnetic moment of electron
$-e$	charge of the electron
Ze	charge of the nucleus
m	electron mass
M	nuclear mass
$\vec{s}$	spin of the electron
$\vec{I}$	nuclear spin
$\vec{L}$	angular momentum operator
$\vec{S}$	operator of the total spin for electrons
n	principal quantum number
l	angular momentum quantum number
j	total angular momentum quantum number
$\{a, b\}$	anticommutator of operators a and b
$[a, b]$	commutator of operators a and b
QED	quantum electrodynamics
NRQED	nonrelativistic QED
HF	Hartree-Fock
hfs	hyperfine splitting
muonium	bound state of antimuon and electron
positronium	bound state of positron and electron
protonium	bound state of proton and antiproton
muonic hydrogen (μH)	bound state of proton and muon
muonic deuterium (μD)	bound state of ^{2}H nucleus and muon
$\bar{p}\,\alpha$	bound state of helium nucleus and antiproton
helion	nucleus of ^{3}He atom

1. Introduction

In this habilitation thesis I summarize and present the main results of the research conducted in the years 2014-2024 following the completion of my PhD. My focus has been on performing highly accurate calculations in the simplest bound-state systems, such as hydrogen or helium. In these simple systems, the usual challenges associated with quantum mechanical calculations are less severe, allowing us to uncover intricate details of the subatomic world. Atomic physics has come a long way since its pioneering days, marked by the exciting confirmation of quantum electrodynamics (QED) through explanations of phenomena like the anomalous magnetic moment of the electron or the Lamb shift in hydrogen. Presently, with the combination of highly precise theoretical calculations and increasingly more accurate experimental data, atomic physics not only serves as a convincing testing ground for QED but also facilitates the precise determination of fundamental constants, and even the nuclear structure properties like the charge radius of the proton.

In general, to enhance our understanding of nature, we can pursue different avenues. One approach involves advancing to higher energies in particle colliders, but this encounters technological, economic, and also political limitations. Another strategy is to delve into the exploration of unknown phenomena, such as dark matter. Alternatively, we can enhance the precision of both theory and experiment wherever feasible. The advantage of the third approach is its considerably lower cost by several orders of magnitude compared to particle accelerators and dark matter searches. This avenue represents a complementary and independent method of searching for new physics since it investigates a completely different scale of energies than particle colliders. The specific motivation for conducting very accurate theoretical calculations lies in several aspects. Firstly, it allows us to test theoretical models and explore the limits of effects that extend beyond them. The comparison between theoretical predictions and experimental data can provide insights into the magnitude of non-renormalizable terms in the QED Lagrangian, and any disparity between theory and experiment could signal the presence of new physics. Secondly, accurate theoretical calculations enable us to determine the nuclear properties of atoms. For example, the hyperfine splitting of energy levels is significantly influenced by the internal structure of the nucleus. Assuming the correctness of theoretical calculations, we can extract values of nuclear parameters from experiments. This could serve to test Quantum Chromodynamics (QCD) and approximate methods of its solution, or to provide us with information about the nuclear structure that is not possible to obtain from QCD. Thirdly, as a byproduct we obtain values of fundamental constants which always have to be inserted into the theoretical predictions. For all these purposes we have to perform the calculations as accurately as possible. To achieve this, we have to take into account various effects of small magnitude, which are often omitted in calculations, either because they are too complicated to evaluate or because the overall precision used in the calculation does not require including terms beyond the nonrelativistic Hamiltonian $H = T + V$. In this thesis, the evaluation of several such effects is presented, and we show that by including them, we reach unparalleled precision of determination of atomic energy levels.

One of the most prominent tests of fundamental physics in atomic systems is derived from the magnetic moment of the electron bound in the hydrogenlike carbon ion. The relative precision of the experiment of 3×10^{-11} [1] is matched by the complementary accuracy of ab initio theoretical calculations based on QED [2]. Experiment and theory are in excellent agreement; their comparison is limited by the uncertainty of the electron mass, as taken from the best electron-trap measurement. In practice, one reverses the problem and determines the electron mass from the bound-electron g-factor, gaining an improvement in accuracy by two orders of magnitude. Another prominent atomic test is determination of the proton charge radius from ordinary (H) and muonic (μH) hydrogen. The lepton universality in the Standard Model states that the coupling constants of the electron and muon are equal, so one must use the same physical laws and constants to predict the energy levels in H and μH. What came out in practice, however, was a surprise. The proton root-mean-square charge radius, treated as an unknown parameter and extracted from the comparison of theory and experiment, turned out to be significantly different for the electronic and muonic spectra (what become known as the proton radius puzzle). As a final example of testing QED we mention determination of the Zemach radius (see definition in Eq. (3.16)) from the hyperfine structure of lithium isotopes ^{6}Li and ^{7}Li. From the comparison of theory and experiment it was determined that the Zemach radius of ^{6}Li is approximately by 40 % smaller than that of ^{7}Li. This was consistently obtained both from Li atom and Li^+ ion using several independent measurements. On the other hand, the results obtained for ^{6}Li from simple models of the nuclear charge and magnetization distribution disagree with this determination by more than 6σ.

To fully appreciate the extensive testing of QED, it is noteworthy to consider the precision achieved in state-of-the-art theoretical calculations for light atoms. For instance, the hyperfine splitting of the $2S$ state in hydrogen was calculated with the relative precision of 2×10^{-9}, reaching sub-Hertz accuracy [3]. On the other hand, the experiment recently reached similar accuracy with relative precision of 5×10^{-9} [4], and is in perfect agreement with theoretical prediction. For $2S - 1S$ transition in hydrogen the theoretical accuracy is even better, reaching 9×10^{-13}, while the experimental accuracy is 4×10^{-15} [5, 6]. For helium, the accuracy of theoretical calculations has been significantly improved in recent years, reaching relative accuracy of 2×10^{-10} [7] for $2S - 2P$ transition, in very good agreement with experiment [8] which has the accuracy of 5×10^{-12}. For helium hyperfine splitting, the theory has achieved a relative accuracy of 6×10^{-9}, whereas the experiment has accuracy of 2×10^{-9} [9, 10]. In all these cases the agreement of theory with experiment is excellent. However, there are also instances of significant disagreement of theory and experimental data. For example, theory for hyperfine splitting in μD is in 5σ tension with experiment [11]. Another case of discrepancy are ionization energies of the 2^3S and 2^3P states in helium, where the disagreement is 6.5σ and 10σ, respectively [12]. Thus, even though QED is the most accurately tested physical theory, there are still some discrepancies that need to be resolved.

The basic estimation of atomic energy levels is derived by solving nonrelativistic Schrödinger equation

$$\hat{H}\psi = E\psi\,. \tag{1.1}$$

For many purposes this is both sufficient approximation and also challenging enough calculation, especially when many-electron atoms and molecules are at play. With approaches like Hartree-Fock (HF) and post-Hartree-Fock methods we are able to tackle the problem of solving the equation (1.1) when no analytical solution is known. However, from a numerical point of view, such calculations are demanding and high-performance computing is needed for their execution.

On the other hand, one- and two-electron systems like hydrogen or helium atoms are much less demanding for numerical evaluation. In particular, nonrelativistic equation for hydrogen is analytically solvable, and for helium it is solvable numerically with arbitrary precision. This allows us to extend the calculations of energy levels beyond the simple nonrelativistic approximation and incorporate relativistic and QED effects. For the hydrogen atom, the fully relativistic determination of energy levels is achieved by solving the Dirac equation

$$\Big(\gamma^\mu \, \Pi_\mu - m\Big)\psi(x) = 0\,, \tag{1.2}$$

and the relativistic corrections are approximately by a factor α^2 smaller than the leading, nonrelativistic result, where α is the fine structure constant [13],

$$\alpha^{-1} = 137.035\,999\,084(21)\,. \tag{1.3}$$

Due to smallness of the fine structure constant the few-electron atoms are loosely bound nonrelativistic systems and the relativistic effects might be treated as perturbations. This can be easily demonstrated by direct calculation of the average velocity of electron in hydrogenlike atom using nonrelativistic wave functions [14],

$$\langle n|\vec{v}^{\,2}|n\rangle = \langle n|\frac{\vec{p}^{\,2}}{m^2}|n\rangle = \frac{(Z\alpha)^2}{n^2}\,, \tag{1.4}$$

where Z is the charge of the nucleus and n is principal quantum number. Thus, as long as Z is small, the nonrelativistic approximation is appropriate. With relativistic effects taken into account, the degeneracy of the nonrelativistic result is partialy removed, as the energies now depend on both the principal quantum number n and the total angular momentum number j.

While the Dirac equation provides theoretical predictions of energy levels that agree better with experiments, it is not the final step in calculations for several reasons. First, the Dirac equation predicts the electron g-factor to be exactly equal to $g = 2$, while experimental observations indicate a slightly larger value due to the anomalous magnetic moment. Second, although the Dirac equation removes some degeneracy, certain energy levels remain degenerate. Notably, it cannot explain the splitting of the $2S_{1/2}$ and $2P_{1/2}$ states in hydrogen, known as the the Lamb shift [15]. And third, Dirac equation (1.2) describes correctly electron bound by infinitely heavy nucleus but completely omits the motion of the nucleus. It is possible to include leading order recoil effects of the order m/M [16] where m is the mass of the electron and M is nuclear mass, but the more general result for arbitrary mass dependence is not known.

These issues are resolved by taking into account the quantum electrodynamics. In QED, the interaction between charged particles is described as the exchange of photons and depicted using so-called Feynman diagrams. In addition to interparticle interaction, QED predicts also self-interaction of the charged particle

with itself, wherein it emits and later absorbs back the virtual photon. Such an effect, known as the self-energy [17, 18, 19], might appear exotic at first glance. However, it has important consequences, as it shifts the energy levels of bound electron in atom by

$$\delta E = e^2 \int \frac{d^4k}{i\,(2\pi)^4\,k^2} \left\langle \gamma^\mu \frac{1}{\gamma\cdot(\Pi-k)-m}\,\gamma^\mu \right\rangle . \tag{1.5}$$

This correction to energy, along with the vacuum polarization [14], constitutes a dominant part of the contributions responsible for splitting of the $2S_{1/2}$ and $2P_{1/2}$ states in hydrogen, consequently explaining the Lamb shift. Feynman diagrams that include internal loops with virtual particles, such as these, are termed radiative corrections. Conversely, diagrams involving photon exchange between two particles without internal loops represent the (nonradiative) recoil contributions. These are important for solving the third issue and accounting for the mass dependence of the nucleus. Of course, it is also possible to combine both types of contributions, which leads to the radiative recoil corrections.

The anomalous magnetic moment of electron can be explained by yet another QED contribution. The leading correction to $g/2-1$ is equal to $\alpha/2\pi$ [20], and its agreement with experiment has proven to be a significant milestone in the acceptance of QED. It is noteworthy that Julian Schwinger, one of the founding fathers of QED, has this result engraved on his tombstone. Including the corrected value of the g-factor into the theoretical formulas for atomic spectra further enhances the agreement with experimental observations.

In our calculations, we employ the approach of the so-called Nonrelativistic quantum electrodynamics (NRQED) [21, 22, 23], which is detailed in the following Chapter. The NRQED method systematically incorporates all nonrelativistic, relativistic, and QED effects, treating the nucleus and electrons on equal footing. This allows us to derive formulas that are applicable for arbitrary electron-to-nucleus mass ratios. Typically, it is sufficient to consider only the first few orders of the mass ratio expansion. Within the NRQED framework we may also account for the influence of the nuclear structure effects on atomic spectra. Given the current experimental and theoretical precision, nuclear effects are non-negligible and must be included in our calculations [14]. This, however, provides an opportunity to gain insights into the internal structure of the nucleus. Additionally, comparing results from scattering experiments with those from various atomic spectra measurements allows us to test the consistency of the theory [24]. Any potential discrepancies observed could be indicative of new physics.

This thesis is organised as follows. In Chapter 2, we provide a brief introduction to the NRQED approach, establishing the explicit form of the expansion of energy levels in powers of the fine structure constant α. Chapter 3 presents the results of our calculations for two-body systems. We explore systems with constituent particles of arbitrary masses, whether pointlike or hadronic, and with spinless or spin-1/2 particles, limiting our study to angular momenta $l \geq 1$. Our objective is to derive a general formula applicable to highly excited states of various systems, including exotic atoms like muonic hydrogen, positronium, or protonium. In the latter part of Chapter 3, we delve into the study of hyperfine structure in hydrogenlike ions. Comparisons between our calculations and experimental measurements allow us to extract contributions to atomic energy

levels arising from nuclear structure effects. Furthermore, by subtracting the corresponding elastic contribution obtained from electron scattering, we determine the nuclear polarizability effect in hydrogenlike $^3He^+$.

Chapter 4 is dedicated to study of heliumlike ions. Firstly, we present the results of our calculation of the higher-order recoil correction to energy levels of helium triplet and singlet states. With the inclusion of this correction, we achieve highly accurate predictions for the $^3He - ^4He$ isotope shift of transitions $2^3S - 2^1S$ and $2^3S - 2^3P$. This can be compared with the experimental data and it allows us to extract the value of the nuclear charge radii difference between these two isotopes of helium. It turns out that the values obtained from different transitions and experiments are in disagreement with each other.

In the subsequent part of Chapter 4, we present our results for the calculation of the α^7 correction to energy levels for helium triplet states. This contribution poses a very challenging calculation but holds significant importance. With the inclusion of this correction, the accuracy of the theory in helium is brought to approximately the same level as in hydrogen. Furthermore, such accuracy allows us to investigate the charge radius of helium with a precision of 10^{-3}, which is relevant in the context of the discrepancy in determining the proton charge radius from ordinary and muonic hydrogen.

In the final part of Chapter 4, we study the hyperfine splitting for heliumlike ions. To achieve this, we calculated the corresponding α^7 contribution to hyperfine splitting of the 2^3S state in ^3He and $^{6,7}Li^+$. In the case of heliumlike lithium, we utilized the outcome of our calculation along with experimental data to extract information about the nuclear structure. The results we obtained are in agreement with the literature, albeit with higher precision. In the case of ^3He atom, we used the comparison of our calculation and the experimental measurement for testing QED, obtaining excellent agreement between theory and experiment. Our theoretical prediction of helium hyperfine structure presents the most accurate theoretical result for non-hydrogenic systems so far.

Finally, Appendix A presents the summary of all the relevant papers in which I am the author or co-author. In Appendix B selected works are included.

2. Theory of energy levels in light atoms

2.1 Nonrelativistic quantum electrodynamics

NRQED is a method first put forward by Caswell and Lepage in [21] and later developed in various works [22, 25, 26, 27]. It is an effective field theory in which nonrelativistic and relativistic momenta scales are treated separately. The initial step involves constructing the NRQED Lagrangian. Subsequently, using Feynman rules and perturbation theory, one can build effective Hamiltonians for interactions. One approach to achieve this is by ensuring that NRQED predictions align with those of QED to the desired order of accuracy in powers of α [21]. Through matching tree diagrams between NRQED and QED, one can determine the corresponding coupling constants in the Lagrangian. This ensures proper consideration of all low-momentum contributions in NRQED. In our approach, we instead derive the NRQED Lagrangian by means of Fouldy-Wouthyusen (FW) transformation of the Dirac Hamiltonian in external electromagnetic field [22], as will be demonstrated below.

QED contributions that involve relativistic momenta in loops are absorbed as renormalizations of the coupling constants for local interactions in NRQED [21]. Given that the wavelengths associated with relativistic momenta are significantly shorter than those with nonrelativistic momenta, the effects due to relativistic loop momenta can be expressed as local interactions. Determining these coupling constants is done through scattering amplitudes in QED.

To illustrate the NRQED method we will first consider ordinary QED theory, starting with Dirac Hamiltonian in the presence of external electromagnetic field,

$$H = \vec{\alpha}\cdot\vec{\pi} + \beta\, m + e\, A^0 = \gamma^0\left[\vec{\gamma}\cdot(\vec{p} - e\vec{A}) + \gamma^0\, e\, A^0 + m\right], \tag{2.1}$$

where $\vec{\pi} = \vec{p} - e\,\vec{A}$. From this Hamiltonian it is possible to obtain many body Lagrangian density by

$$\mathcal{L} = \sum_a \psi_a^*\,(i\partial_t - H)\,\psi_a + \mathcal{L}_{\rm EM} = \sum_a \bar{\psi}_a\left(\gamma^\mu\,(p^\mu - e\,A^\mu) - m\right)\psi_a + \mathcal{L}_{\rm EM}\,, \tag{2.2}$$

where $\mathcal{L}_{\rm EM}$ is a Lagrangian of the electromagnetic field, and $\bar{\psi}_a = \psi_a^*\,\gamma_0$. It follows from this expression that the conserved electromagnetic four-current of the particle a is

$$j_a^\mu = e\,\bar{\psi}_a\gamma^\mu\,\psi_a\,. \tag{2.3}$$

Now we utilize the formalism of Feynman rules for constructing the QED theory and evaluating individual contributions given by Feynman diagrams. The interaction between charged particles is established through the exchange of photons. For the interaction vertex given by the four-current (2.3) we get the rule

$$j_a^\mu \to ie\,\gamma^\mu\,. \tag{2.4}$$

Now, for instance, the previously mentioned self-energy contribution is given by the expression

$$\delta E = e^2 \int \frac{d^4k}{i\,(2\pi)^4} \frac{g^{\mu\nu}}{k^2} \Big\langle \psi \Big| \gamma^0 \gamma^\mu \, e^{i\vec{k}\cdot\vec{r}} \frac{1}{(E - H - k^0)} \, e^{-i\vec{k}\cdot\vec{r}} \, \gamma^0 \gamma^\nu \Big| \psi \Big\rangle \,, \tag{2.5}$$

which we rewrote into slightly different form and assumed that the state in the consideration is stationary. It is evident that the rule for interaction vertex, derived from the electromagnetic current, could already be extracted from the Dirac Hamiltonian (2.1) as the term coupled to the four-potential A^μ. The expression in Eq. (2.5) represents the exact QED expression for the one-loop self-energy to all orders in $Z\alpha$.

Now we turn to the derivation of the low-momentum part of NRQED, deferring the treatment of relativistic momenta for later. The main idea is to carry out the nonrelativistic expansion directly for the Dirac Hamiltonian before constructing the NRQED Lagrangian density, electromagnetic current, and the rules for vertices. Instead of the expression (2.3), we obtain a nonrelativistic expansion for the current, which is then employed with Feynman rules. Since the current is now in the form of a series, numerous individual Feynman diagrams need to be considered. For example, exchange of two photons between particles in full QED is given by two diagrams, one ordinary and one with crossed photon lines. In NRQED, this transforms into various other diagrams, each involving the exchange of two photons with different expressions at the interaction vertices. Each such a diagram contributes to a different order in α. It is crucial to note that every Feynman diagram in NRQED contributes only to single order in α. This systematic approach allows for the comprehensive collection of all relevant diagrams, ensuring a complete contribution that agrees with QED at every order in α. The expressions for individual NRQED contributions are also much simpler to evaluate compared to those in full QED.

Detailed derivation of NRQED Lagrangian is presented in [22] or in our work [28]. The key concept involves utilizing the FW transformation of the Dirac Hamiltonian to decouple the upper and lower components of the Dirac wave function up to a specified order in the $1/m$ expansion, leading to a nonrelativistic expansion of the Hamiltonian H. The result of the transformation is the FW Hamiltonian $H_{\rm FW}$ defined as

$$H_{\rm FW} = e^{i\,S} \, (H - i\,\partial_t) \, e^{-i\,S} \,, \tag{2.6}$$

where S is unitary operator. The choice of the unitary transformation operator S, and consequently the resulting FW Hamiltonian, is not unique. We use the operator S defined as

$$\begin{aligned} S = \; & -\frac{i}{2\,m} \Big[\beta\,\vec{\alpha}\cdot\vec{\pi} - \frac{1}{3\,m^2}\,\beta\,(\vec{\alpha}\cdot\vec{\pi})^3 + \frac{\beta}{5\,m^4}\,(\vec{\alpha}\cdot\vec{\pi})^5 + \frac{i\,e}{2\,m}\,\vec{\alpha}\cdot\vec{E} - \frac{\beta\,e}{4\,m^2}\,\vec{\alpha}\cdot\partial_t\vec{E} \\ & + \frac{i\,e}{24\,m^3}\,[\vec{\alpha}\cdot\vec{\pi},[\vec{\alpha}\cdot\vec{\pi},\vec{\alpha}\cdot\vec{E}]] - \frac{i\,e}{3\,m^3}\Big((\vec{\alpha}\cdot\vec{\pi})^2\,\vec{\alpha}\cdot\vec{E} + \vec{\alpha}\cdot\vec{E}\,(\vec{\alpha}\cdot\vec{\pi})^2 \Big) \Big] \,. \end{aligned} \tag{2.7}$$

This choice allows us to eliminate undesired higher-order terms that are odd in matrix $\vec{\alpha}$ (or, equivalently, in matrix γ^j) and that mix the upper and lower components of the wave function. Because the operator S is not unique, the FW

Hamiltonian $H_{\rm FW}$ we obtain might be different from the one obtained through the standard textbook approach. This difference might be expressed by a transformation involving some additional even operator. However, all variants of the FW Hamiltonian are equivalent at the level of matrix elements, ensuring they lead to the same physical results.

It might be advantageous to perform further unitary transformations to simplify the FW Hamiltonian H_{FW} and transform it into a form that si more suitable for a particular calculation. Examples of such further transformation are given by operators

$$S' = -\frac{e}{16m^3}\{\vec{\sigma}\cdot\vec{\pi}, \vec{\sigma}\cdot\vec{E}\}\,, \tag{2.8}$$

which removes the time derivative of electric field, or

$$S'' = \frac{e}{8m^2}\,\sigma^{ij}\,\{A^i\,,\,\pi^j\}\,, \tag{2.9}$$

which removes the perpendicular part of the electric field $\vec{E}_\perp = -\partial_t\vec{A}$. Here, the spin operator σ^{ij} is defined as

$$\sigma^{ij} = \frac{1}{2\,i}[\sigma^i, \sigma^j]\,. \tag{2.10}$$

The FW Hamiltonian that we finally obtain is thus

$$\begin{aligned} H_{\rm FW} = {} & eA^0 + \frac{\pi^2}{2m} - \frac{e}{4m}\sigma^{ij}B^{ij} - \frac{\pi^4}{8m^3} + \frac{e}{16m^3}\Big(\sigma^{ij}B^{ij}\,\vec{\pi}^2 + \vec{\pi}^2\,\sigma^{ij}B^{ij}\Big) \\ & - \frac{e}{8m^2}\Big(\vec{\nabla}\cdot\vec{E}_\parallel + \sigma^{ij}\{E^i_\parallel, \pi^j\}\Big) + \frac{e^2}{8m^3}\vec{E}^2 - \frac{e^2}{16m^3}B^{ij}B^{ij} - \frac{e^2}{4m^2}\sigma^{ij}A^iE^j \\ & + \frac{ie}{16m^3}[\sigma^{ij}\{A^i, \pi^j\}, \pi^2] - \frac{e^2}{8m^3}A^i\,\nabla^jB^{ij} + \frac{p^6}{16\,m^5} + \dots\,, \end{aligned} \tag{2.11}$$

where dots stand for omitted higher order terms. The magnetic field tensor is $B^{ij} = \partial^i A^i - \partial^j A^i$, longitudal part of the electric field is $\vec{E}_\parallel = -\vec{\nabla}A^0$, and $\nabla^i \equiv \nabla_i = \partial/\partial x^i$. This FW Hamiltonian is particulary suitable for derivation of the α^7 correction to energy levels in heliumlike atom [28]. For other cases it may be advantageous to utilize the Hamiltonian in slightly different forms by applying additional transformations.

Having obtained the FW Hamiltonian, we proceed to construct the many-body Lagrangian density in a similar manner as in full QED, using the first equality in Eq. (2.2) with $H = H_{FW}$. Subsequently, we construct the current operator and rules for interaction vertices. Employing the Feynman formalism, we derive expressions for diagrams corresponding to the exchange of photons between particles, each proportional to a specific power of the fine structure constant α. This process enables the systematic calculation of contributions to various orders in α within the framework of NRQED.

In the treatment of radiative corrections, for example in our work [29], it is advantagous to incorporate dominant part of the radiative corrections from the outset. This is achieved by modifying the Dirac Hamiltonian to include electromagnetic form factors F_1 and F_2:

$$\begin{aligned} H = {} & \vec{\alpha}\cdot\left[\vec{p} - e\,F_1(\vec{\nabla}^2)\,\vec{A}\right] + \beta\,m + e\,F_1(\vec{\nabla}^2)\,A_0 \\ & + F_2(\vec{\nabla}^2)\,\frac{e}{2\,m}\,\left(\mathrm{i}\,\vec{\gamma}\cdot\vec{E} - \frac{\beta}{2}\,\Sigma^{ij}\,B^{ij}\right)\,, \end{aligned} \tag{2.12}$$

instead of using the Hamiltonian (2.1). Here, $\Sigma^{ij} = \frac{\mathrm{i}}{2}[\gamma^i, \gamma^j]$. This Hamiltonian (2.12) is used as the starting point for the analysis, and the subsequent procedures would follow a similar line as before.

Before proceeding with the evaluation of individual NRQED contributions to energy levels, let us discuss the high-momentum part of NRQED. This part arises from the exchange of virtual photons with relativistic momenta $k \approx m$, which consequently impart large momentum also to interacting charged particles in virtual states. Having large momenta means that their wavelengths are very short and the overlap of the wavefunctions of interacting particles is essentialy only when they are in contact. As a result, this contribution is given by a local Dirac-δ-like interaction.

Splitting of QED into contributions from different momentum scales introduces singularities into the theory that need to be addressed. To handle these singularities properly, a regulator has to be included in the calculations. The choice of a specific regularization method is arbitrary, but dimensional regularization has been found to be particularly suitable. The relativistic momentum contribution serves as a renormalization of the coupling constants for local interactions, removing the singularities from the calculation and ensuring that the theory remains mathematically well-defined.

The high-momentum contribution can be obtained from the scattering amplitude for the exchange of two and more photons between particles in full QED. The advantage of dimensional regularization is that, when separating different momentum scales, one does not split the integration over photon momentum into several integration regions. The integration is always performed over whole range of photon momenta k, and the separation is done by rescaling the *integration variable* k. For instance, if we are interested in the region $k \approx \alpha\, m$, we rescale all photon momenta in the expression for the scattering amplitude as $\vec{k} \to \alpha\, \vec{k}$, $k^0 \to \alpha\, k^0$. The momenta of incoming and outgoing fermions are always rescaled as $\vec{p} \to \alpha\, \vec{p}$. After this rescaling, the integrand of the scattering amplitude is expanded up to a particular order in α, and integration is performed over all possible photon momenta $\int dk^D/(2\pi)^D$. To obtain the high-momentum contribution, we rescale only fermion momenta $\vec{p} \to \alpha\, \vec{p}$ since photon momentum is of the order $k \approx m$. Following the expansion in α and integration, we get the desired high-momentum contribution. This procedure is demonstrated in our paper [28] where the high-energy part of order α^7 was derived from the scattering amplitude for the exchange of two photons between electrons. Using the scattering amplitude from full QED, it is also possible to check the NRQED contribution from the region of $k \approx m\alpha$, as was demonstrated in that paper. It serves as an important check of the consistency of NRQED method.

2.2 Higher-order effective Hamiltonian

With the help of perturbation theory, we proceed to calculate the Green functions. We consider the equal-time retarded Green function G, which in the stationary case is $G = G(t - t')$, where t and t' are the common time of the *out* and the *in* electrons, correspondingly. The Fourier transform over the time variable $t - t'$

yields the propagator in the energy-coordinate representation,

$$G(E) = \frac{1}{E - H_0 - \Sigma(E)},$$

where H_0 is the Schrödinger-Coulomb Hamiltonian of an N-electron atom,

$$H_0 = \sum_a \frac{p_a^2}{2\,m_a} + V,\ H_0|\phi\rangle = E_0|\phi\rangle\,. \tag{2.13}$$

H_0 may either include the nucleus as a dynamic particle or it is assumed that the nucleus is a static source of the Coulomb field. The operator $\Sigma(E)$ incorporates various relativistic and QED corrections like the photon exchange correction, the electron and photon self-energy etc.,

$$\begin{aligned} G(E) = &\frac{1}{E - H_0} + \frac{1}{E - H_0}\,\Sigma(E)\,\frac{1}{E - H_0} \\ &+ \frac{1}{E - H_0}\,\Sigma(E)\,\frac{1}{E - H_0}\,\Sigma(E)\,\frac{1}{E - H_0} + \ldots\,. \end{aligned} \tag{2.14}$$

The energy level of a bound state can be interpreted as a pole of $G(E)$ as a function of E. We now consider the matrix element of G between the nonrelativistic wave function ϕ that corresponds to this level. This correspondence is always present because relativistic and QED effects are considered small perturbations to the system. The matrix element is

$$\begin{aligned} \langle\phi|G(E)|\phi\rangle &= \frac{1}{E - E_0} + \frac{1}{(E - E_0)^2}\,\langle\phi|\Sigma(E)|\phi\rangle \\ &\quad + \frac{1}{(E - E_0)^2}\,\langle\phi|\Sigma(E)\,\frac{1}{E - H_0}\,\Sigma(E)|\phi\rangle + \ldots \\ &= \frac{1}{E - E_0 - \sigma(E)}\,, \end{aligned} \tag{2.15}$$

where

$$\sigma(E) = \langle\phi|\Sigma(E)|\phi\rangle + \langle\phi|\Sigma(E)\,\frac{1}{(E - H_0)'}\,\Sigma(E)|\phi\rangle + \ldots\,. \tag{2.16}$$

Here, the prime in $(E - H_0)'$ means that we are excluding the reference state from the resolvent. The resulting bound-state energy E (i.e. the position of the pole) is

$$E = E_0 + \sigma(E_0) + \sigma(E_0)\,\frac{\partial\sigma(E_0)}{\partial E_0} + \ldots\,. \tag{2.17}$$

In most cases the explicit dependence of Σ on the reference state (through E_0) can be eliminated by means of various commutation identities. The only exception is the so-called Bethe logarithm and higher-order corrections to it. If we consider these terms separately then the operator Σ gives an effective Hamiltonian

$$H = H_0 + \Sigma \equiv H_0 + H^{(4)} + H^{(5)} + H^{(6)} + H^{(7)} + \ldots \tag{2.18}$$

from which the corrections to energy levels are calculated. The calculation of terms $H^{(j)}$ follows from Feynman rules for Lagrangian $\mathcal{L}$, and each term is of the order α^j with $H_0 \equiv H^{(2)}$. Derivation of the effective Hamiltonians $H^{(j)}$ is the

central issue of NRQED method. While the derivation of the leading order contributions is rather simple, the higher-order contributions require collection and evaluation of significant amount of diagrams. NRQED necessarily involves more interactions than QED, but the advantage lies in the simplicity of their evaluation. The NRQED method allows for the systematic inclusion of all relativistic and QED effects order by order.

It is advantageous to use the photon propagator in the Coulomb gauge, as it allows us to conveniently arrange individual contributions by the order of α to which they contribute. The photon propagator $G_{\mu\nu}(k)$ in the Coulomb gauge is given by:

$$G_{\mu\nu}(k) = \begin{cases} -\frac{1}{\vec{k}^2}\,, & \mu=\nu=0, \\ \frac{-1}{k_0^2-\vec{k}^2+i\epsilon}\left(\delta_{ij}-\frac{k_i k_j}{\vec{k}^2}\right), & \mu=i,\ \ \nu=j\,. \end{cases} \tag{2.19}$$

We consider separately the contributions due to Coulomb G_{00} and transverse G_{ij} photon exchange, as they contribute at different order of α. It follows from the Feynman formalism that the typical one-photon exchange contribution between electrons a and b (or similarly between electron and nucleus) is

$$\begin{aligned}\langle\phi|\Sigma(E_0)|\phi\rangle = e^2\int\frac{d^4k}{(2\pi)^4\,i}G_{\mu\nu}(k)\Bigg\langle\phi\Bigg|j_a^\mu(k)e^{i\vec{k}\cdot\vec{r}_a}\frac{1}{E_0-H_0-k^0+i\epsilon}\,j_b^\nu(-k)e^{-i\vec{k}\cdot\vec{r}_b} \\ + j_b^\mu(k)e^{i\vec{k}\cdot\vec{r}_b}\frac{1}{E_0-H_0-k^0+i\epsilon}\,j_a^\nu(-k)e^{-i\vec{k}\cdot\vec{r}_a}\Bigg|\phi\Bigg\rangle\,,\end{aligned} \tag{2.20}$$

where ϕ is an eigenstate of H_0, and $j_a^\mu(k)$ is NRQED electromagnetic current operator of the particle a, whose exact form is obtained from the NRQED Lagrangian density derived from FW Hamiltonian (2.11). The current operator is derived similarly to full QED, as the coefficient multiplying the polarization vector ϵ^μ in the annihilation part of the electromagnetic potential A^μ,

$$A^\mu(\vec{r},t) \sim \epsilon_\lambda^\mu\, e^{i\vec{k}\cdot\vec{r}-ik^0t}\,\hat{a}_\lambda + \text{H.c.} \tag{2.21}$$

Since the FW Hamiltonian in Eq. (2.11) and, consequently, also the Lagrangian are in the form of nonrelativistic expansion, the same also holds for the current operator $j_a^\mu(k)$. The first terms of the expansion of j^0 component from Eq. (2.11) (i.e. terms involving coupling to A^0) are

$$j^0(\vec{k}) = 1 + \frac{i}{4m^2}\,\sigma^{ij}\,k^i\,p^j - \frac{1}{8m^2}\,\vec{k}^2 + \dots\,, \tag{2.22}$$

and for the $\vec{j}$ component (i.e. terms involving coupling to $\vec{A}$) are

$$j^i(\vec{k}) = \frac{p^i}{m} + \frac{i}{2m}\,\sigma^{ij}\,k^j + \dots\,. \tag{2.23}$$

Inserting different terms of these expansions into interaction vertex will lead to contributions of different order in α. Some contributions of a particular order in α can be calculated in the so-called nonretardation approximation. In such a case, one sets $k^0 = 0$ in the photon propagator $G_{\mu\nu}(k)$ and in $j(k)$ since these terms would lead to corrections of a higher order in α. Thus, the only dependence on

k^0 is, in this case, left in the fermion propagator. To resolve it, symmetrization $k^0 \leftrightarrow -k^0$ is used in order to make the integral finite. The integral is then

$$\frac{1}{2}\int \frac{dk^0}{2\,\pi\,i}\left[\frac{1}{E_0 - H_0 - k^0 + i\epsilon} + \frac{1}{E_0 - H_0 + k^0 + i\epsilon}\right] = -\frac{1}{2}\,. \tag{2.24}$$

Thus, the one-photon exchange contribution in nonretardation approximation is then

$$\langle\phi|\Sigma(E_0)|\phi\rangle = \, -e^2 \int \frac{d^3k}{(2\pi)^3} G_{\mu\nu}(k^0 = 0, \vec{k}) \langle\phi| j_a^\mu(\vec{k}) e^{i\vec{k}\cdot(\vec{r}_a - \vec{r}_b)}\, j_b^\mu(-\vec{k})|\phi\rangle\,. \tag{2.25}$$

Two comments are in place now. Firstly, in the integration with respect to k^0 we assumed that $H_0 - E_0$ is positive, which holds when ϕ is the ground state. For excited states, the integration contour is deformed in such a way that all the poles from the electron propagator lie on one side, so it is not strictly speaking the Feynman contour. The result for k^0 integration for excited states is the same however, leading to Eq. (2.25). Secondly, it is possible to generalize the expression in Eq. (2.20) to $D = d + 1$ dimensions instead of $D = 4$. This is convenient when deriving higher-order effective Hamiltonians $H^{(j)}$ for $j \geq 5$ which contain singular parts that need to be regularized. In dimensional regularization, all the expressions are transformed from $d = 3$ spatial dimensions into d-dimensional form. After canceling all the singularities, the final expression is transformed back into $d = 3$, and numerical evaluation is then performed.

It is easy to see that the leading order contribution from G_{00} in Eq. (2.25) is the Coulomb interaction. However, this is already part of the Hamiltonian H_0 and thus we have to exclude it from the nonrelativistic expansion. The next-order terms coming from j^0 and $\vec{j}$ lead to the so-called Breit-Pauli Hamiltonian $H^{(4)}$ and represent the leading relativistic corrections. In Hamiltonian $H^{(5)}$, the leading QED corrections start to contribute. For that, one has to include also the two-photon exchange between particles, and retardation correction to one-photon exchange. In our works [24, 28, 29, 30, 31, 32, 33, 34, 35] we derived higher-order QED contributions of order α^6 and α^7 which will be presented in the following Chapters.

2.3 Perturbation expansion of energy levels

Once the NRQED effective Hamiltonians are acquired, the energy levels can be expressed as a power series in powers of the fine structure constant α,

$$E = E^{(2)} + E^{(4)} + E^{(5)} + E^{(6)} + E^{(7)} + \dots\,, \tag{2.26}$$

where $E_0 \equiv E^{(2)}$ and $E^{(j)}$ is of the order α^j. Every term in the expansion (2.26) is obtained as an expectation value of the corresponding effective Hamiltonian with the nonrelativistic wave function ϕ, which is the eigenfunction of the non-relativistic Hamiltonian H_0 with energy E_0. The leading relativistic correction is the expectation value of the Breit-Pauli Hamiltonian,

$$E^{(4)} = \langle\phi|H^{(4)}|\phi\rangle\,. \tag{2.27}$$

The next-order contribution is a sum of the expectation value of the effective Hamiltonian $H^{(5)}$ and the low-energy contribution $E_L^{(5)}$,

$$E^{(5)} = \langle\phi|H^{(5)}|\phi\rangle + E_L^{(5)}\,, \tag{2.28}$$

where $E_L^{(5)}$ is given by the Bethe logarithm [14],

$$E_L^{(5)} = -\frac{2\,\alpha}{3\,\pi\,m_a\,m_b}\,\langle\phi|\vec{P}\,(H_0 - E_0)\,\ln\left[\frac{H_0 - E_0}{\alpha^2\,\mu}\right]\vec{P}|\phi\rangle\,, \tag{2.29}$$

where m_a and m_b are masses of particles a and b, μ is the reduced mass, and $\vec{P} = \sum \vec{p}_i$. The series in Eq. (2.26) is not analytical in α, and starting from $E^{(5)}$, the individual contributions may include powers of $\ln\alpha$.

Higher-order QED correction $E^{(6)}$ is again sum of two parts, namely

$$E^{(6)} = \langle\phi|H^{(6)}|\phi\rangle + \langle\phi|H^{(4)}\frac{1}{(E_0 - H_0)'}\,H^{(4)}|\phi\rangle\,. \tag{2.30}$$

Both terms in the latter equation separately contain singularities. In order to get finite contribution to the energy level, the singularities have to be isolated by a means of regularization. When the singular parts of both terms are combined together, they algebraically cancel each other, and the resulting expression is finite.

Finally, the contribution $E^{(7)}$ can be written as

$$E^{(7)} = \langle\phi|H^{(7)}|\phi\rangle + 2\,\langle\phi|H^{(4)}\frac{1}{(E_0 - H_0)'}\,H^{(5)}|\phi\rangle + E_L^{(7)}\,, \tag{2.31}$$

where $E_L^{(7)}$ presents relativistic corrections to Bethe logarithm.

It is possible to perform one more perturbation expansion of every term $E^{(i)}$, namely, one may expand it in powers of the electron to nucleus mass ratio,

$$E^{(i)} = E^{(i,0)} + \frac{m}{M}\,E^{(i,1)} + \left(\frac{m}{M}\right)^2 E^{(i,2)} + \ldots\,. \tag{2.32}$$

The leading order corresponds to the nonrecoil approximation when the nucleus is infinitely heavy, and the following terms correspond to recoil corrections. In our papers [24, 28, 29, 30, 31, 33] we calculated the energy levels of helium atom up to the third order recoil correction $E^{(2,3)}$, the second order recoil correction $E^{(4,2)}$, the leading order recoil corrections $E^{(5,1)}$ and $E^{(6,1)}$, and nonrecoil correction $E^{(7,0)}$. For two-body systems such as hydrogenlike atoms or positronium atom, we obtained general result for states with total angular momentum $l > 0$ that is valid for arbitrary mass ratio of the constituent particles up to the order α^6 [35].

In the following Chapters we will present the results of our calculations for two-body systems (and in particular for hydrogenlike atoms), and for heliumlike atoms.

3. Hydrogenlike atoms

For two-body systems such as hydrogen, muonic hydrogen, muonium, or positronium, theoretical calculations provide the most accurate QED predictions [14]. The hydrogen atom, being the simplest atomic system, represents an ideal testing ground for the boundaries of validity of QED. One of the important tests is comparison of the Lamb shift in ordinary hydrogen and in muonic hydrogen, where the electron is replaced by the muon. In both of these systems the comparison of theory with experimental data can be used for determination of the proton charge radius. Proton is not a pointlike particle but has internal structure and finite charge radius, which manifests in the leading order as a correction to the Coulomb potential of the nucleus. This, in turn, results in a shift of atomic energy levels, which depends on the value of the proton charge radius. This shift, and therefore also the value of the charge radius, can be determined from the difference between theoretical prediction for a pointlike nucleus and experimental data for transitions between different levels. Interestingly, results from ordinary and muonic hydrogen significantly disagreed with each other, which became known in the literature as the proton charge radius puzzle [37, 38, 39], and attracted interest of physics community since such a discrepancy might have been a signal of new physics. Subsequent measurements have brought the two results closer into agreement by adjusting the hydrogenic result towards the muonic hydrogen value [40, 41]. The comparison of theory and experiment for hydrogen also allows for the determination of the Rydberg constant. The uncertainty of the Rydberg constant is currently given by the theory of hydrogen Lamb shift and makes it one of the most accurately determined fundamental constants.

3.1 Effective Hamiltonian of two-body system

Here, we will present our results for the effective NRQED Hamiltonians and corrections to energy levels up to the order α^6 for two-body systems with arbitrary masses of the constituents [35]. These results are valid for both spinless and spin-1/2 particles, with the restriction on angular momenta $l \geq 1$.

The nonrelativistic Hamiltonian H_0 for two particles with charges e_1, e_2, and masses m_1, m_2, in the center of mass frame ($\vec{p} = \vec{p}_1 = -\vec{p}_2$), is

$$H_0 = \frac{\vec{p}^{\,2}}{2\,\mu} + \frac{e_1\,e_2}{4\,\pi}\,\frac{1}{r}\,, \tag{3.1}$$

where $\mu = m_1 m_2/(m_1 + m_2)$ is the reduced mass, and $r = |\vec{r}| = |\vec{r}_1 - \vec{r}_2|$. Setting $e_1 = -e, e_2 = Z\,e$, the nonrelativistic energy $E^{(2)}$ in the state with principal quantum number n is

$$E^{(2)} = E_0 = -\frac{(Z\,\alpha)^2\,\mu}{2\,n^2}\,. \tag{3.2}$$

All the higher order corrections to energy are calculated using the expectation values with eigenfunctions of H_0.

3.1.1 Leading relativistic and QED corrections

The next-order contribution represents the leading relativistic corrections, which are of the order α^4. It can be obtained from the Feynman diagram with single transverse $G_{ij}(k)$ or Coulomb $G_{00}(k)$ photon exchange, and is given by the Breit-Pauli Hamiltonian [35, 42]

$$\begin{aligned} H^{(4)} = & -\frac{\vec{p}^{\,4}}{8\,m_1^3} - \frac{\vec{p}^{\,4}}{8\,m_2^3} + \frac{e_1\,e_2}{4\,\pi}\left\{\frac{1}{2\,m_1\,m_2}\,p^i\left(\frac{\delta^{ij}}{r}+\frac{r^i\,r^j}{r^3}\right)p^j + \frac{g_1\,g_2}{4\,m_1\,m_2}\left[\frac{s_1^i\,s_2^j}{r^3}\right.\right. \\ & \left.\times\left(\delta^{ij}-3\,\frac{r^i\,r^j}{r^2}\right) - \frac{8\,\pi}{3}\,\vec{s}_1\cdot\vec{s}_2\,\delta^3(\vec{r})\right] - \frac{\vec{r}\times\vec{p}}{2\,r^3}\cdot\left[\frac{g_1}{m_1\,m_2}\,\vec{s}_1+\frac{g_2}{m_1\,m_2}\,\vec{s}_2\right. \\ & \left.\left.+\frac{(g_2-1)}{m_2^2}\,\vec{s}_2+\frac{(g_1-1)}{m_1^2}\,\vec{s}_1\right]\right\} - \frac{e_1 e_2}{6}\Big(\big\langle r_E^2\big\rangle_1+\big\langle r_E^2\big\rangle_2\Big)\,\delta^3(\vec{r})\,. \end{aligned} \tag{3.3}$$

Here, $\vec{r}=\vec{r}_1-\vec{r}_2$, $\vec{s}_a$ is the spin of particle a, g_a is the g-factor related with magnetic moment anomaly by $g_a = 2\,(1+\kappa_a)$, and $\langle r_E^2\rangle_a$ is the square of the charge radius. For a spinless particle it is $\langle r_E^2\rangle = g = 0$. The Hamiltonian (3.3) does not encompass contributions due to potential annihilation effects, as would be present in positronium, nor does it consider strong interaction effects inherent in hadronic particles.

From the Hamiltonian in Eq. (3.3) one obtains $E^{(4)}$ by calculating the expectation value with the nonrelativistic eigenfunction of H_0. The result for a state with the principal quantum number n and the angular momentum l is

$$\begin{aligned} E^{(4)} = & \mu^3(Z\alpha)^4\left\{\frac{1}{8\,n^4}\left(\frac{3}{\mu^2}-\frac{1}{m_1\,m_2}\right) - \frac{1}{\mu^2(2l+1)\,n^3} + \frac{2\,\delta_{l0}}{3\,n^3}\Big(\big\langle r_E^2\big\rangle_1+\big\langle r_E^2\big\rangle_2\Big)\right. \\ & + \frac{\delta_{l0}}{m_1\,m_2\,n^3} + \frac{2}{l(l+1)(2l+1)n^3}\left[\langle\vec{L}\cdot\vec{s}_1\rangle\left(\frac{1+2\kappa_1}{2m_1^2}+\frac{1+\kappa_1}{m_1 m_2}\right)\right. \\ & \left.\left. + \langle\vec{L}\cdot\vec{s}_2\rangle\left(\frac{1+2\kappa_2}{2m_2^2}+\frac{1+\kappa_2}{m_1 m_2}\right) - \frac{6(1+\kappa_1)(1+\kappa_2)}{m_1 m_2\,(2\,l-1)(2\,l+3)}\langle s_1^i s_2^j (L^i L^j)^{(2)}\rangle\right]\right. \\ & \left. + \frac{8\,\delta_{l0}}{3 m_1 m_2\,n^3}(1+\kappa_1)(1+\kappa_2)\,\langle\vec{s}_1\cdot\vec{s}_2\rangle\right\}. \end{aligned} \tag{3.4}$$

In the last equation we have introduced a symmetric traceless tensor $(L^iL^j)^{(2)}$, which is defined as

$$(L^iL^j)^{(2)} = \frac{1}{2}\Big(L^iL^j+L^jL^i\Big) - \frac{\delta^{ij}}{3}\vec{L}^2\,. \tag{3.5}$$

Expression (3.4) is valid for arbitrary spin of both particles, pointlike or with finite size.

For the next-order contribution we restrict the investigation only to non-S-states. This enables us to omit local δ-like terms which contribute only for the states with $l=0$. QED effects for $l>0$ are partially accounted for in the g-factor, which is present in the Breit-Pauli Hamiltonian $H^{(4)}$. Additional QED corrections are represented as $E^{(5)}$, and for $l>0$ they have the well known form

[44]

$$E^{(5)} = -\frac{7}{3\pi}\frac{(Z\alpha)^5\mu^3}{m_1 m_2}\frac{1}{l(l+1)(2l+1)\,n^3} - \frac{4}{3\pi}\left(\frac{1}{m_1}+\frac{Z}{m_2}\right)^2\frac{\alpha(Z\alpha)^4\mu^3}{n^3}\,\ln[k_0(n,l)]\,, \tag{3.6}$$

where $\ln[k_0(n,l)]$ is the Bethe logarithm

$$\ln[k_0(n,l)] \equiv \frac{n^3}{2\mu^3(Z\alpha)^4}\left\langle \phi \left| \vec{p}\,(H_0-E_0)\ln\left[\frac{2(H_0-E_0)}{\mu(Z\alpha)^2}\right]\vec{p}\right|\phi\right\rangle . \tag{3.7}$$

Bethe logarithm needs to be evaluated numerically, depends on the energy of the reference state, and its values for various states have been tabulated.

3.1.2 Higher-order QED correction

Now we turn to the QED contribution of the order α^6, given by Eq. (2.30). For the case of two pointlike spin-1/2 particles with angular momentum $l = 0$ and arbitrary masses the calculation was performed in [45]. Here, we present our results for states with angular momentum $l \geq 1$. For these states, there is a notable simplification in the calculations. The singularities present in both terms of Eq. (2.30) are solely proportional to a local δ-like interaction, which is nonzero only for S states. Consequently, by confining ourselves to states with higher angular momentum, we can eliminate all problematic terms and circumvent the need for any form of regularization. The general results valid for arbitrary masses and for both pointlike and hadronic particles can be used for excited states of exotic atoms, such as antiproton bound to helium nucleus. For highly excited states of these atoms the contact interaction, e.g. from strong force, is negligible. If corresponding measurements are available, this presents an opportunity for the precise determination of fundamental constants or tests of the existence of unknown long-range interactions, similarly to precision tests performed with antiprotonic helium [46, 47, 48], but much more accurate.

In our calculation we neglected (electronic) vacuum polarization, which can be included separately. The significance of this contribution depends on particular n, l, and constituent masses. In our work [35] we derived the complete effective operator $H^{(6)}$ for spinless or spin-1/2 particles for states with $l > 1$, and in [36] we extended the calculation also to states with $l = 1$. The expression for the operator $H^{(6)}$ is lengthy and can be expressed as a sum of several terms,

$$H^{(6)} = \sum_{i=0\ldots9}\delta H_i\,, \tag{3.8}$$

where the individual contributions come from various Feynman diagrams corresponding to the exchange of Coulomb or transverse photons between particles, and are presented in [35, 36].

For the second-order term in Eq. (2.30), we use the Breit Hamiltonian from Eq. (3.3) with the contact terms omitted. Evaluating the expectation values using hydrogenic wave functions and combining the second-order contribution

with the expectation value of $H^{(6)}$, we obtain the complete result for $E^{(6)}$. It can be expressed in the form

$$E^{(6)} = (Z\alpha)^6 \left[A + B \langle \vec{L} \cdot \vec{s}_1 \rangle + C \langle \vec{L} \cdot \vec{s}_2 \rangle + D \langle \vec{s}_1 \cdot \vec{s}_2 \rangle + F \langle (L^i L^j)^{(2)} s_1^i s_2^j \rangle \right], \tag{3.9}$$

where the individual coefficients A, B, C, D, F are presented in [35, 36]. The general formulas for arbitrary masses are quite complicated, but the special cases yield more compact results. For instance, in the case of infinitely heavy nucleus, the result for $E^{(6)}$ reduces to the well-known result from the Dirac equation if the orbiting particle has spin-1/2 [35]. In the case of a spinless orbiting particle, the result concurs with the one derived from the Klein-Gordon equation. The first-order recoil correction again agrees with the one in the literature for spin-1/2 particle, while for a spinless particle, the recoil correction has not been calculated previously.

The energy (3.9) can also be checked against the known result for positronium atom by setting $m_1 = m_2$, $Z = 1$, $\kappa_1 = \kappa_2 = 0$, and both particles are considered pointlike. Our result aligns with a prior calculation in Ref. [49] for $l > 1$. However, we have found that there is a mistake in all the previous calculations in the literature for $l = 1$ state [36]. In particular, there is a discrepancy for orthopositronium $j = 0$ state, arising from an incorrect calculation of contact terms. In our work [36], we provide a corrected theoretical result for positronium that rectifies this mistake. It is important to note that the numerical impact of this correction is negligible and does not significantly affect the comparison with experimental data, which is inherently less accurate.

In our publication [36], we employed the general formulas to derive the fine structure of $2P$ states in light muonic atoms, specifically focusing on the case of muonic helium ions. Previous QED calculations for the $2P$ fine structure of μHe ions were conducted in Refs. [50, 51], neglecting higher-order terms in the muon-to-nucleus mass ratio. Our calculation incorporates the complete dependence on the mass ratio, and the resulting expression for $\mu^3\mathrm{He}^+$ is

$$E_{\mathrm{fs}}(\text{our work}) = 144.785(3)\,\mathrm{meV}\,, \tag{3.10}$$
$$E_{\mathrm{fs}}(\text{theo}) = 144.785(5)\,\mathrm{meV}\,[50]\,, \tag{3.11}$$
$$E_{\mathrm{fs}}(\text{exp}) = 144.763(114)\,\mathrm{meV}\,[52]\,, \tag{3.12}$$

and for $\mu^4\mathrm{He}^+$ it is

$$E_{\mathrm{fs}}(\text{our work}) = 146.182(3)\,\mathrm{meV}\,, \tag{3.13}$$
$$E_{\mathrm{fs}}(\text{theo}) = 146.181(5)\,\mathrm{meV}\,[51]\,, \tag{3.14}$$
$$E_{\mathrm{fs}}(\text{exp}) = 146.047(96)\,\mathrm{meV}\,[53]\,, \tag{3.15}$$

The result in Eq. (3.9) is the most general formula for two-body systems with $l \geq 1$. Its utility extends beyond conventional systems like hydrogenlike ions; it can also be applied to more exotic atoms such as pionic helium, hydrogenlike helium, or muonic and antiprotonic atoms. This highlights that precise measurements of energy levels can serve not only for determining fundamental constants

but also for probing unknown interactions in a range not accessible in normal atoms, namely, from 1 up to 100 MeV. Although there are no definite plans to study rotational states of, for example, protonium or $\bar{p}\,\alpha$, the availability of a high-precision theoretical result is crucial for planning the corresponding measurements.

As a final note let us remark that for hydrogenlike atoms we presented the summary of contributions to the Lamb shift in our review paper [5].

3.2 Hyperfine structure of hydrogenlike ions

The interaction between the magnetic moment of the nucleus and that of the electron results in the splitting of atomic energy levels, a phenomenon known as hyperfine splitting (hfs). Measurements of the hfs in atoms have achieved exceptional accuracy, with the ground state of hydrogen experimentally known up to 12 digits [54, 55]. This makes hfs an excellent candidate for high precision tests of bound-state QED, and for searches of physics beyond the Standard Model of fundamental interactions [56].

The hfs in atoms and ions is determined not only by the value of nuclear magnetic moment but also by the distribution of the charge and the magnetic moment over the nucleus, as well as the nuclear vector polarizability. At the present time, these effects cannot be accurately calculated and thus present the main source of uncertainty in theoretical calculations.

The nuclear structure effects are usually divided into the elastic and inelastic parts. The elastic part is expressed in terms of charge and magnetic form factors, whereas the dominant inelastic effect is nuclear polarizability. It is well known that the dominant hfs nuclear effect is of the elastic kind, and is proportional to the so-called Zemach radius [57],

$$r_Z = \int d^3r_1 \int d^3r_2\, \rho_E(\vec{r}_1)\, \rho_M(\vec{r}_2)\, |\vec{r}_1 - \vec{r}_2|\,, \tag{3.16}$$

which is the convolution of electric and magnetic form factors ρ_E and ρ_M.

The nuclear polarizability is largely unknown due to the complexity of its theoretical description. The effect is most pronounced for muonic deuterium hfs where it is supposed to be as large as the elastic effect. However, theoretical predictions are in conflict with experiment [11, 58]. For electronic atoms, the nuclear polarizability is less significant than for muonic atoms but nevertheless still not completely negligible. Even for hydrogen the inelastic effects were shown to yield about 5% of the elastic effect contribution [59].

In the absence of theoretical calculations, we determine the nuclear polarizability from experimental hfs splitting [60]. We use the fact that all relativistic and QED effects for point nucleus can be calculated with high accuracy, and that the elastic form factors of the nucleus can be extracted from scattering experiments. Instead of Zemach radius from Eq. (3.16), we introduce *effective* Zemach radius $\widetilde{r}_Z$, which incorporates inelastic nuclear contributions and can be accurately determined from high-precision experiments for hfs splitting. On the other hand, the standard elastic Zemach radius r_Z was determined from the electron-scattering data by Sick [61]. The difference $\widetilde{r}_Z - r_Z$ then gives us the result for nuclear polarizability correction, which we are otherwise unable to obtain by

direct calculation. From the comparison of the nucleur structure obtained for different isotopes or ions, we may test the consistency of our calculations and experimental measurements.

The leading hfs splitting of $1S$ state in hydrogenlike atom is given by the so-called Fermi splitting,

$$E_F = \frac{8}{3}(Z\alpha)^4 \frac{\mu^3}{m\,M}\,(1+\kappa)\,, \tag{3.17}$$

where Z and M are the nuclear charge number and the mass, respectively, μ is the reduced mass of the atom, and $\kappa = (g-2)/2$ is the nuclear magnetic moment anomaly, with the natural nuclear g-factor defined as

$$\vec{\mu}_M = \frac{Z\,e}{2\,M}\,g\,\vec{I}\,. \tag{3.18}$$

Here, $\vec{\mu}_M$ and $\vec{I}$ are the magnetic moment and the spin of the nucleus, respectively. The complete hfs splitting can be conveniently expressed as

$$E_{\rm hfs} = E_F\,(1+\delta)\,, \tag{3.19}$$

where δ represents the correction to the Fermi splitting due to relativistic, QED, and nuclear effects. Within the approach of the NRQED, δ is represented as an expansion in terms of the fine-structure constant α,

$$\delta = \kappa_e + \delta^{(2)} + \delta^{(3)} + \delta^{(4)} + \delta^{(1)}_{\rm nuc} + \delta^{(1)}_{\rm rec} + \delta^{(2)}_{\rm nuc} + \delta^{(2)}_{\rm rec}\,, \tag{3.20}$$

where κ_e is the magnetic moment anomaly of the free electron, $\kappa_e = \alpha/(2\pi) + O(\alpha^2)$, and $\delta^{(i)}$, $\delta^{(i)}_{\rm nuc}$, and $\delta^{(i)}_{\rm rec}$ are the QED, nuclear, and recoil corrections of order α^i, respectively. The overview of individual parts of the δ coefficient in Eq. (3.20) is presented in our work [60]. The advantage of this representation is that the δ coefficients in different atomic states are strongly correlated. Therefore, one can employ an experimental hfs value measured for one state in order to obtain an improved theoretical prediction for another state.

The inelastic contribution emerges already in the term $\delta^{(1)}_{\rm nuc}$, which is a sum of the elastic contribution proportional to the Zemach radius r_Z, and the nuclear polarizability contribution. We now define the effective Zemach radius as

$$\delta^{(1)}_{\rm nuc} = -\,2\,Z\,\alpha\,\mu\,\widetilde{r}_Z\,, \tag{3.21}$$

thus formally encompassing both elastic and inelastic parts. In our work [60] we determined $\delta^{(1)}_{\rm nuc}$ for hydrogenlike ion $^3{\rm He}^+$ by taking the difference of the experimental hfs value from Ref. [62] and the theoretical prediction without $\delta^{(1)}_{\rm nuc}$. Our result for the effective Zemach radius is

$$\widetilde{r}_Z = 2.600(8)\,{\rm fm}\,, \tag{3.22}$$

which is in agreement with but more accurate than the previous determination

$$\widetilde{r}_Z = 2.608(24)\,{\rm fm}\,[62]\,. \tag{3.23}$$

The difference of the effective Zemach radius and the elastic Zemach radius obtained in Ref. [61] from the electron-scattering data yields $\widetilde{r}_Z - r_Z = 0.072(18)\,{\rm fm}$.

We interpret this difference as the contribution of the nuclear polarizability. The nuclear polarizability effect in $^3He^+$ is thus surprisinly small, only about 3% of the elastic effect. This is smaller than in the hydrogen where the inelastic hfs contribution is about 5% [59]. This is unexpected since helion, being a composite nucleus, is relatively weekly bound system as compared to proton. This can be illustrated by comparing the proton mean excitation energy of 400 MeV (i.e. the average energy needed to excite the proton from its ground state within an atomic nucleus) with the proton separation energy for helion nucleus, which is 5 MeV. The nuclear polarizability is expected to be roughly proportional to the inverse of these energies. Indeed, for the Lamb shift the corresponding energy shifts are $-0.109(12)$ kHz and $-55(5.5)$ kHz, for hydrogen and $^3He^+$, respectively. However, for the hfs the expected relation between hydrogen and He^+ fails entirely. At the present time we do not have any explanation why for helion the inelastic hfs nuclear contribution is smaller than for proton.

As previously mentioned, we can use the nuclear structure effects determined for $^3He^+$ ion to enhance the theoretical prediction of hfs in ^3He atom. With high accuracy, the nuclear structure contribution expressed using δ coefficients is the same for both $^3He^+$ and ^3He. Thus, by using the value extracted from $^3He^+$, we eliminate the dominant uncertainty in ^3He hfs. In Chapter 4, we will demonstrate that this approach leads to a significant improvement of the theoretical result. On the other hand, using the nuclear structure contribution extracted from heliumlike Li^+ we obtain theoretical prediction for hydrogenlike Li^{2+}. Specifically, we utilize the results for nuclear structure extracted from Li^+ measurements to determine the hyperfine structure of Li^{2+} isotopes using the known hydrogenic theory for a pointlike nucleus [34],

$$E_{\rm hfs}(^6Li^{2+}) = 8.479\,190\,(21)\,\text{GHz}\,, \tag{3.24}$$

$$E_{\rm hfs}(^7Li^{2+}) = 29.855\,013\,(86)\,\text{GHz}\,. \tag{3.25}$$

Details about evaluation of the nuclear structure of heliumlike Li^+ are presented in the next Chapter. So far, there is no experimental data for Li^{2+}. It is remarkable that the uncertainty of our prediction for the Li^{2+} hfs comes exclusively from the uncertainty of the Li^+ hfs measurement.

4. Heliumlike atoms

Heliumlike atoms represent the simplest few-electron systems. Unlike hydrogenic systems, heliumlike atoms lack analytical solutions for nonrelativistic wave functions, necessitating the use of numerical methods to determine energy levels. However, by variational optimization of the wave function, we can obtain the expectation values of required operators with arbitrary precision [63]. The accuracy of theoretical predictions for energy levels is, in principle, restricted only by the order of the NRQED Hamiltonians considered. This means that not only hydrogenlike but also heliumlike atoms can be used for tests of QED. For instance, the high-precision experimental data can be used for setting contraints on spin-dependent forces between electrons that go beyond the Standard Model of fundamental interactions [64]. Another application is the determination of the nuclear charge radius and the comparison with results from muonic atoms and electron scattering. This becomes significant in the context of the proton radius puzzle in hydrogen. The first step towards such a comparison is the recent muonic helium experiment [65], which determined the charge radius of the helium-4 nucleus with a 0.05% precision. However, to extract the value of the charge radius with sufficient accuracy, theoretical calculations within the NRQED framework need to include corrections to energy up to the order α^7, i.e. up to the contribution in Eq. (2.31). For helium, it is also necessary to include the finite nuclear mass through the series (2.32), i.e. include recoil corrections proportional to powers of electron to nucleus mass ratio m/M.

As with hydrogenlike atoms, we present the contribution to energy levels and hyperfine splitting for heliumlike atoms. In our works [30, 31] we calculated the recoil correction to energy levels of the order $\alpha^6\, m/M$ for singlet and triplet states of helium. With these results, we can determine the nuclear charge radii differences between two isotopes of helium [24]. To obtain the absolute value of the helium charge radius, we calculated the nonrecoil contribution of the order α^7 in series of papers [7, 28, 29, 33] for helium triplet states. While our results are in perfect agreement with experimental data for $2^3S - 2^3P$ transition, the ionization energies of individual states significantly disagree with experiment. This discrepancy has been confirmed in recent experimental measurements [12]. The source of this tension between theory and experiment is currently unknown. However, the agreement of our theoretical predictions with experimental results for the $2^3S - 2^3P$ transition extends to heliumlike ions as well [66, 67].

For hyperfine splitting in ^{3}He atoms, we conducted the calculation up to the order α^7 [9]. Utilizing the results for nuclear structure obtained from hydrogenlike $^3He^+$, we achieved theoretical predictions that are in perfect agreement with experimental data. Additionally, we extended the calculation to $^{6,7}Li^+$ to determine nuclear structure effects and test the consistency of hyperfine structure results between $^{6,7}Li^+$ ion and ^{6,7}Li atom [34]. We confirmed that the nuclear structure obtained from the comparison of theory and experiment in these systems is in very good agreement.

4.1 Numerical calculations for two-electron systems

In two-electron systems, we are unable to solve the Schrödinger equation analytically. Therefore, we resort to numerical methods to obtain the nonrelativistic wave function and energy. To do so, we follow the approach of Korobov [63] and expand the spatial part of the helium wave function in a basis set of exponential functions of the form

$$\phi_i(r_1, r_2, r_{12}) = e^{-\alpha_i r_1 - \beta_i r_2 - \delta_i r_{12}} \pm (r_1 \leftrightarrow r_2)\,, \tag{4.1}$$

and

$$\vec{\phi}_i(r_1, r_2, r_{12}) = \vec{r}_1\, e^{-\alpha_i r_1 - \beta_i r_2 - \delta_i r_{12}} \pm (r_1 \leftrightarrow r_2)\,, \tag{4.2}$$

for the S and P states, respectively. Nonlinear parameters α_i, β_i and δ_i are obtained in the process of the basis optimization. The advantage of this basis set lies in its ability to provide a closed-form expression for the master integral

$$\frac{1}{16\,\pi^2}\int d^3r_1 \int d^3r_2\, \frac{e^{-\alpha r_1 - \beta r_2 - \delta r_{12}}}{r_1\, r_2\, r_{12}} = \frac{1}{(\alpha+\beta)(\beta+\gamma)(\gamma+\alpha)}\,, \tag{4.3}$$

and the results converge rapidly with an increase in the size of the basis set. For example, considering the ground state of helium, we obtain the nonrelativistic energy

$$E_0(1S) = -2.903\,724\,377\,, \tag{4.4}$$

by employing 300 basis functions. In the case of a basis set comprising 1500 functions, we would attain the 17-digit accuracy for the nonrelativistic energy E_0, which is sufficient for the current experimental accuracy.

For relativistic and QED corrections, the expectation values of the first-order operators $\langle H^{(j)}\rangle$ are simplified by applying various operator identities and the Schrödinger equation. This simplification leads to a combination of expectation values of basic irreducible operators Q_i,

$$Q_1 = 4\pi\delta^3(r_1)\,, \tag{4.5}$$
$$Q_2 = 4\pi\delta^3(r_{12})\,, \tag{4.6}$$
$$Q_3 = 4\pi\delta^3(r_1)/r_2\,, \tag{4.7}$$
$$\ldots$$

where the full list of Q_i operators with $i = 1 \ldots 64$ is presented in [7]. Review of methods for numerical calculations with exponential basis is summarized in our paper [73], along with the details for numerical evaluation of the second-order contributions and the Bethe logarithm.

4.2 Energy levels

The nonrelativistic energy for helium atom was calculated in various works, see e.g. [63]. Derivation of the leading relativistic and QED effects for helium is presented e.g. in [23, 68]. The higher-order QED corrections of order α^6 were

calculated for helium singlet and triplet states in [23, 69]. The Breit Hamiltonian $H^{(4)}$ which enters the α^6 contribution through the second-order term (i.e. the second term in Eq. (2.30)) needs to be used in dimensionally-regularized form [29],

$$\begin{aligned} H^{(4)} = & -\frac{\pi\,\alpha}{m^2}\,\delta^d(r) + \sum_{a=1,2}\left\{-\frac{p_a^4}{8\,m^3} + \frac{\pi\,Z\alpha}{2\,m^2}\,\delta^d(r_a)\right\} - \frac{\alpha}{2\,m^2}\,p_1^i\left[\frac{\delta^{ij}}{r} + \frac{r^i\,r^j}{r^3}\right]_\epsilon p_2^j \\ & - \frac{\pi\,\alpha}{d\,m^2}\,\sigma_1^{ij}\,\sigma_2^{ij}\,\delta^d(r) + \sum_{a=1,2}\frac{1}{4\,m^2}\,\sigma_a^{ij}\left(\nabla_a^i V\right)p_a^j + \frac{1}{4\,m^2}\,\sigma_1^{ik}\,\sigma_2^{jk} \\ & \times\left(\nabla^i\,\nabla^j - \frac{\delta^{ij}}{d}\,\nabla^2\right)\left[\frac{\alpha}{r}\right]_\epsilon - \frac{1}{2\,m^2}\left(\sigma_1^{ij}\,\nabla^i\left[\frac{\alpha}{r}\right]_\epsilon p_2^j - \sigma_2^{ij}\,\nabla^i\left[\frac{\alpha}{r}\right]_\epsilon p_1^j\right), \end{aligned} \tag{4.8}$$

where $d = 3 - 2\epsilon$ is the dimension of the space, and $[x]_\epsilon$ stands for the notation for d-dimensional form of the operator x. For instance, Coulomb potential in d-dimensional form is given by

$$V(r) = \int \frac{d^dk}{(2\pi)^d}\,\frac{4\pi}{k^2}\,e^{i\vec{k}\cdot\vec{r}} = \pi^{\epsilon-1/2}\,\Gamma(1/2-\epsilon)\,r^{2\epsilon-1} \equiv \left[\frac{1}{r}\right]_\epsilon. \tag{4.9}$$

The effective Hamiltonian $H^{(6)}$ is also expressed in d-dimensional form. When both contributions in Eq. (2.30) are combined, all the singular parts cancel each other. Consequently, the nonrecoil contribution $E^{(6,0)}$, for which the mass M of the nucleus is infinitely heavy, is finite.

In papers [70, 71], we calculated energy levels and fine structure splitting for nD states of helium with $n = 3\ldots6$, utilizing the existing theory and incorporating the nonrecoil contribution $E^{(6,0)}$. We found out that the nonradiative contribution of the order α^6, which had been previously omitted for D states, is more significant and of opposite sign than the radiative contribution. This leads to 10σ difference from previous theoretical results [72]. This was a surprising result since, typically, radiative corrections are much more significant than nonradiative contributions. In our work [32] we extended the calculation of the nonrecoil contribution $E^{(6,0)}$ to arbitrary light atoms with N electrons.

Finally, for S and P states, it is necessary to include also the recoil correction $E^{(6,1)}$ and nonrecoil correction $E^{(7,0)}$ to obtain a sufficiently accurate theoretical prediction and extract the value of the nuclear charge radius from the comparison with experiment. In the following we will present the results of our derivation of these corrections.

4.2.1 Contribution of the order $\alpha^6\,m/M$

The leading recoil correction $E^{(6,1)}$ is smaller by a factor of m/M compared to the contribution $E^{(6,0)}$ and, in general, can be expressed as

$$\begin{aligned} E^{(6,1)} = & \,\delta_M\langle\phi|H^{(4)}\frac{1}{(E_0-H_0)'}\,H^{(4)}|\phi\rangle + \delta_M\langle H^{(6)}\rangle + 2\,\langle\phi|H_M^{(4)}\frac{1}{(E_0-H_0)'}\,H^{(4)}|\phi\rangle \\ & + \langle H_M^{(6)}\rangle\,. \end{aligned} \tag{4.10}$$

Here, $\delta_M\langle x\rangle$ represents the perturbation of the expectation value of the operator x by the nuclear kinetic energy $\vec{P}^2/2M$ in the wave function, nonrelativistic Hamiltonian and nonrelativistic energy. Furthermore, $H_M^{(4)}$ and $H_M^{(6)}$ are additional recoil operators of the order α^4 and α^6, originating from the interaction between the nucleus and electrons. Their explicit form for singlet and triplet states of helium is presented in our papers [30, 31].

The second-order contributions in Eq. (4.10) contain divergencies coming from the summation over the intermediate states. They arise when operators on the left and on the right of the resolvent $1/(E_0-H_0)'$ are sufficiently singular, so that their first-order matrix elements are finite but the second-order matrix elements diverge. Example of such a operator is the Dirac δ-function. The divergences become more tractable if one moves them to first-order matrix elements. This can be done by expressing the corresponding operator as an anticommutator of Hamiltonian H_0 with a function of Coulomb potentials, plus some more regular operator. In particular, we write the Breit Hamiltonian as

$$H^{(4)} = \{H_0 - E_0, Q\} + H_R^{(4)}\,, \tag{4.11}$$

where $H_R^{(4)}$ is regular operator whose second-order matrix element is finite, and

$$Q = \alpha\left[\frac{Z}{r_1}+\frac{Z}{r_2}\right]_\epsilon + \beta\left[\frac{1}{r}\right]_\epsilon\,, \tag{4.12}$$

where α, β are some coefficients. The corresponding second-order expression with $H^{(4)}$ is thus rewritten as

$$\begin{aligned}\langle\phi|H^{(4)}\frac{1}{(E_0-H_0)'}\,H^{(4)}|\phi\rangle = \langle\phi|H_R^{(4)}\frac{1}{(E_0-H_0)'}\,H_R^{(4)}|\phi\rangle + \langle Q\,(H_0-E_0)\,Q\rangle \\ + 2\,\langle H^{(4)}\rangle\,\langle Q\rangle - \langle\{H^{(4)},Q\}\rangle\,.\end{aligned} \tag{4.13}$$

The singularities, which are proportional to ϵ^{-1}, are thus transferred to the first-order terms, where they can be algebraically canceled out by other first-order contributions. Similar treatment is used also for the third term in Eq. (4.10). After this is done, we set $d=3$ in the final formulas.

We present results for the so-called centroid energies, which are defined as the average over all fine and hyperfine energy sublevels,

$$E(2^{2S+1}L) \;=\; \frac{\sum_{J,F}(2\,F+1)\,E(2^{2S+1}L_{J,F})}{(2\,I+1)\,(2\,S+1)\,(2\,L+1)}\,, \tag{4.14}$$

where ${}^{2S+1}L$ denotes the state with the angular momentum L and the spin S. The results for the α^6 leading recoil correction $E^{(6,1)}$ for singlet and triplet states of ^{4}He derived in our works [30, 31] are

$$E^{(6,1)}(1^1S) = -347.79\,\mathrm{kHz}\,, \tag{4.15}$$

$$E^{(6,1)}(2^1S) = -21.56\,\mathrm{kHz}\,, \tag{4.16}$$

$$E^{(6,1)}(2^1P) = -2.82\,\mathrm{kHz}\,, \tag{4.17}$$

$$E^{(6,1)}(2^3S) = -29.91\,\mathrm{kHz}\,, \tag{4.18}$$

$$E^{(6,1)}(2^3P) = -1.11\,\mathrm{kHz}\,. \tag{4.19}$$

We also calculated higher-order recoil corrections $E^{(2,2)}$, $E^{(2,3)}$, and $E^{(4,2)}$ for both singlet and triplet states, as their inclusion is necessary in our level of precision [30, 31]. With these corrections taken into account, it is possible to obtain theoretical prediction for the ^{3}He-^{4}He isotope shift of transitions 2^3S-2^3P and 2^3S-2^1S, for which accurate experimental data exists. This, in turn, enables us to extract the value of nuclear charge radii difference $\delta r^2 \equiv r^2(^3\mathrm{He}) - r^2(^4\mathrm{He})$ from the comparison with experiment, as the difference of theoretical calculation and experimental data is [24]

$$\delta E = C\,\delta r^2\,, \tag{4.20}$$

with C being the coefficient which is calculated from theory. For isotope shift, the next order correction to energy, i.e. the correction $E^{(7,0)}$, is the same for both isotopes and thus canceled out. Only the recoil correction would $E^{(7,1)}$ contribute. The theory is then sufficient to obtain the nuclear charge radii difference with uncertainty 1% or better. The results obtained by comparing our calculation with various experiments are

$$\delta r^2(2^3S - 2^1S)[74] = 1.027\,(11)\ \mathrm{fm}^2 \tag{4.21}$$

$$\delta r^2(2^3S - 2^3P)[75] = 1.069\,(3)\ \mathrm{fm}^2\,, \tag{4.22}$$

$$\delta r^2(2^3S - 2^3P)[76] = 1.061\,(3)\ \mathrm{fm}^2\,. \tag{4.23}$$

Surprisingly, contradictory results have been obtained between the determination of radii difference using the results from 2^3S-2^3P transition and from 2^3S-2^1S transition. Obviously, the nuclear charge radius has to be the same, provided that no new physics is involved. Numerically dominating part of theoretical calculations was checked against independent calculations of Drake and coworkers [72], and the difference in calculations cannot explain the 4σ discrepancy between the results for δr^2. The unexplained discrepancy thus calls for the verification of the experimental results.

4.2.2 Contribution of the order α^7

Contribution to the energy levels of the order α^7 is given by Eq. (2.31). We performed the calculation in the nonrecoil approximation and restricted ourselves only to triplet states. For triplet states, the wave function vanishes at the point $r_1 = r_2$, which means that a great deal of singular terms proportional to contact interaction $\delta^3(r_{12})$ do not contribute. This results in a significant simplification of the calculation. Nevertheless, the complete evaluation of the α^7 contribution was significant undertaking, and we had to split the project into several parts, which were calculated separately in a series of papers over the course of three years for helium and another two years for heliumlike ions. The calculation consists of three parts: i) relativistic corrections to the Bethe logarithm (3.7), ii) radiative corrections, and iii) nonradiative corrections coming from the photon exchange between electrons.

The first part comes from the relativistic corrections to the Bethe logarithm. The leading-order Bethe logarithm of the order α^5 for helium is

$$E_L^{(5)} \;=\; \frac{e^2}{m^2}\int_{k<\Lambda}\frac{d^3k}{(2\,\pi)^3\,2\,k}\left(\delta^{ij}-\frac{k^i\,k^j}{k^2}\right)\left\langle P^i\,\frac{1}{E_0-H_0-k}\,P^j\right\rangle\,, \tag{4.24}$$

where $\vec{P} = \vec{p}_1 + \vec{p}_2$. Dependence on the high-momentum cutoff Λ is removed when one combines $E_L^{(5)}$ with the corresponding high-momentum contributions.

Calculation of the relativistic corrections of the order α^7 to Eq. (4.24) was presented in our paper [33]. It can be splitted into three parts:

$$E_L^{(7)} = E_{L1} + E_{L2} + E_{L3}\,. \tag{4.25}$$

Here, E_{L1} represents the contribution resulting from the perturbation of the wave function, nonrelativistic energy, and nonrelativistic Hamiltonian in the expression (4.24) by the Breit Hamiltonian $H^{(4)}$. Furthermore, E_{L2} is induced by the relativistic correction to the current operator $\vec{P}$, and the third part, E_{L3}, is the retardation correction beyond the dipole approximation. From an analytical point of view, the derivation of $E_L^{(7)}$ is simple. The main difficulty lies in the numerical evaluation of individual parts in Eq. (4.25). For the perturbation of the Bethe logarithm by Breit Hamiltonian, we again use regularization (4.11), and we subtract the large-k asymptotics of integrands [33]. Apart from helium ($Z = 2$), we have derived the results for relativistic Bethe logarithms for heliumlike ions up to $Z = 12$ [77]. Moreover, the extrapolation of our results for large Z is in excellent agreement with the analytical values obtained from the hydrogen theory.

The second part of the $E^{(7)}$ contribution to helium energy stems from radiative corrections and is examined in our paper [29]. These corrections arise from the self-energy and the vacuum polarization. It is a sum of the first-order and the second-order contributions,

$$E_{\rm rad}^{(7)} = \langle H_{\rm rad}^{(7)} \rangle + 2 \left\langle H^{(4)} \, \frac{1}{(E_0 - H_0)'} \, H_{\rm rad}^{(5)} \right\rangle , \tag{4.26}$$

where $H_{\rm rad}^{(j)}$ is radiative part of the effective Hamiltonian of the order α^j. To partially incorporate the radiative corrections, we include the electromagnetic form factors into H_{FW}, as indicated in Eq. (2.12). This modification affects the interactions between electrons through the anomalous magnetic moment and the slopes of the form factors $F_1'(0)$ and $F_2'(0)$. The remaining parts come from the integration over the photon momenta $k > \Lambda$ in the low-energy region (the relativistic corrections to Eq. (4.24)), the middle-energy region where both the radiative and exchanged photons are of the order $m\alpha$, and the remaining contributions from the high-energy region not accounted for by the form factors. To encompass all these terms, a considerable number of various Feynman diagrams must be considered [29].

In our calculation we employed further simplification by exploiting the fact that for hydrogenlike atoms the correction $E^{(7)}$ is known. Therefore, in our calculation, we neglected some of the local terms, namely those that are proportional to $Z^3\,\delta^3(r_a)$, $a = 1, 2$. These terms can be reintroduced in the final step of the calculation by adjusting the hydrogenic limit of our formulas to match the known results for hydrogen from the literature. The advantage of this approach is that it enables us to omit large amount of singular contributions and avoid explicit calculation of some of the high-energy contributions. However, electron-electron singularities that remain still need to be addressed using dimensional regularization formalism. The final formula is finite, however, and may be again expressed using Q_i operators, as was presented in Ref. [29]. It was explicitly verified that

both the singularities proportional to $1/\epsilon$ and the dependence on the photon momentum cutoff Λ cancel out in the results.

The last part of the $E^{(7)}$ contribution comes from the nonradiative photon exchange between particles, which we derived in Ref. [28]. It is of the form

$$E^{(7)}_{\rm exch} = \left\langle H^{(7)}_{\rm exch} \right\rangle + 2 \left\langle H^{(4)} \, \frac{1}{(E_0 - H_0)'} \, H^{(5)}_{\rm exch} \right\rangle , \tag{4.27}$$

where $H^{(j)}_{\rm exch}$ is an effective Hamiltonian of the order j coming from the nonradiative photon exchange. Once again, various energy scales and Feynman diagrams contribute to the final result. In this part, a direct comparison with hydrogenic results is not feasible. The only simplification arises from the fact that, for triplet states, the local interaction proportional to the electron-electron Dirac delta function vanishes. To obtain the high-energy part, it was necessary to evaluate the two-photon exchange scattering amplitude in full QED. The collection and evaluation of all the individual terms contributing to $E^{(7)}_{\rm exch}$ is challenging and lengthy but the final formula, as presented in [28], is relatively simple and compact.

Numerical results for all three parts of the contribution $E^{(7)}$ are presented in our paper [7]. For 2^3S state, the obtained contribution to ionization (centroid) energy of ^{4}He is $-6.168(1)$MHz, while for 2^3P state it is $2.280(1)$MHz. By collecting all the individual corrections to the energy levels, we get the total theoretical prediction for transition frequencies between various triplet states in helium:

$$E_{\rm theo}(2^3S - 3^3D_1) = 786\,823\,849.540\,(52)\text{MHz}\,, \tag{4.28}$$
$$E_{\rm theo}(2^3P_0 - 3^3D_1) = 510\,059\,754.863\,(16)\text{MHz}\,, \tag{4.29}$$
$$E_{\rm theo}(2^3P - 2^3S) = 276\,736\,495.620\,(54)\text{MHz}\,. \tag{4.30}$$

The uncertainty is mainly given by the estimate of unknown α^8 correction, based on hydrogenic result. Our results may be compared with experiment [78, 79, 8],

$$E_{\rm exp}(2^3S - 3^3D_1) = 786\,823\,850.002\,(56)\text{MHz}\,, \tag{4.31}$$
$$E_{\rm exp}(2^3P_0 - 3^3D_1) = 510\,059\,755.352\,(28)\text{MHz}\,, \tag{4.32}$$
$$E_{\rm exp}(2^3P - 2^3S) = 276\,736\,495.600\,0\,(14)\text{MHz}\,. \tag{4.33}$$

From the comparison, it is evident that we achieve excellent agreement for intrashell $2^3P - 2^3S$ transition, but there is notable disagreement for transitions with different n. This disagreement was confirmed in recent work [12], where the ionization energy of the 2^1S state was measured. In combination with experimental data for $2^3S - 2^1S$ and $2^3S - 2^3P$ transitions, the ionization energies of 2^3S and 2^3P states were derived. These experimental ionization energies exhibit 6.5σ and 10σ disagreement with theoretical prediction. The source of this discrepancy is unknown at the moment, but a possible explanation could involve some unknown theoretical contribution that shifts both 2^3S and 2^3P states by approximately the same value.

In our paper [67], we extended the calculation to heliumlike ions with nuclear charge Z up to $Z = 12$ and derived theoretical predictions for the $2^3S - 2^3P_J$ transition. For $Z = 3, 4, 5$ we compared our results to known experimental data, finding agreement with the exception for Be^{2+} [80]. It should be noted, however, that this measurement was already reported to disagree with theoretical predictions for the fine structure, which calls for an independent verification of this

experiment. Furthermore, for $5 \leq Z \leq 30$, we combined NRQED method with $1/Z$ expansion in our work [66]. The method based on $1/Z$ expansion, sometimes referred to as "all-order approach", is a completely different approach for calculation of the energy levels [81]. In this method, all orders of electron-nucleus binding strength $Z\alpha$ are included and one expands in powers of the electron-electron interaction parameter $1/Z$. This approach is suited for heavier ions where $1/Z$ is converging quickly, while the NRQED expansion cannot be used as $Z\alpha$ is no longer small. Problematic is the region around $Z \approx 10$ where both methods face difficulties, requiring a combination of both of them to obtain the most accurate results. We verified that for $Z = 5$, the results obtained by both approaches are consistent with each other, namely the effects of the order α^7 which were rigorously calculated using NRQED approach are in agreement with those derived from fitting the all-order results [67].

Recently, there was a measurement of $2^3S - 2^3P_J$ transition in heliumlike carbon $^{12}C^{4+}$ [82]. This isotope is ideal for testing QED since it has no nuclear spin, and its nuclear charge radius is well known from electron scattering and muonic atom spectroscopy. The results of the measurement

$$E_{\rm exp}(2^3S - 2^3P_0) = 1\,316\,052.219\,3(19)\,\text{GHz}\,, \tag{4.34}$$
$$E_{\rm exp}(2^3S - 2^3P_1) = 1\,315\,677.192\,8(17)\,\text{GHz}\,, \tag{4.35}$$
$$E_{\rm exp}(2^3S - 2^3P_2) = 1\,319\,748.571\,4(17)\,\text{GHz}\,, \tag{4.36}$$

turned out to be in excellent agreement with our theoretical prediction from [66],

$$E_{\rm theo}(2^3S - 2^3P_0) = 1\,316\,052.03(27)\,\text{GHz}\,, \tag{4.37}$$
$$E_{\rm theo}(2^3S - 2^3P_1) = 1\,315\,677.60(75)\,\text{GHz}\,, \tag{4.38}$$
$$E_{\rm theo}(2^3S - 2^3P_2) = 1\,319\,748.55(13)\,\text{GHz}\,. \tag{4.39}$$

This serves as a further test of both the consistency of our results and the estimate of their uncertainty. The comparison of theoretical prediction and the measurement [82] was used for determination of the carbon charge radius, and the result is consistent with previous determinations.

4.3 Hyperfine structure of heliumlike ions

For atomic ^{4}He, the nuclear spin vanishes, and no hyperfine splitting occurs. Therefore, to study hfs in helium, we need to investigate the case of the ^{3}He isotope, where the nuclear spin is nonzero. The measurement of the 2^3S state hfs of ^{3}He is very accurate [10], providing an excellent test of QED theory. The leading hfs contribution is of the order α^4 and is given by the Fermi splitting. For helium it reads

$$E_F \equiv \langle V_F \rangle = \frac{4\,\pi\,Z\alpha}{3\,m\,M}\,g\,\langle \vec{I}\cdot[\vec{s}_1\,\delta^3(r_1) + \vec{s}_2\,\delta^3(r_2)]\rangle\,. \tag{4.40}$$

The complete hfs of helium can be expressed in the same form like in the case of hydrogen,

$$E_{\rm hfs} = E_F\,(1 + \kappa_e + \delta^{(2)} + \delta^{(3)} + \delta^{(4)} + \delta_{\rm nuc} + \delta_{\rm rec}) \equiv E_F\,(1+\delta)\,. \tag{4.41}$$

The individual δ coefficients in Eq. (4.41) for helium are correlated with those for hydrogenlike ion. Thus, to obtain helium hfs, it is advantageous to write the δ coefficient as a sum of two parts,

$$\delta(\mathrm{He}) = \delta(\mathrm{He}^+) + \delta(\mathrm{He\text{-}He}^+)\,. \tag{4.42}$$

The first part, $\delta(\mathrm{He}^+)$, can be extracted from the experiment on He^+ ion, encompassing, among other factors, contributions steming from nuclear structure. The second part is the difference between hydrogenlike and heliumlike results and has to be calculated theoretically. Only a limited number of terms contribute to this difference, as outlined in our paper [9]. Specifically, the QED corrections of the order $\alpha^2\,E_F$, $\alpha^3\,E_F$, and recoil corrections due to hyperfine mixing of 2^3S and 2^1S states must be calculated for helium. The first of them is known in the literature [83]. The QED contribution of the order α^7 was calculated by us in Ref. [9]. Its derivation is similar to calculation of the correction $E^{(7)}$ to energy centroid, with the difference that only the relativistic correction to Bethe logarithm and radiative corrections are nonvanishing. Photon exchange terms do not contribute at this order. To evaluate radiative corrections, we employed a similar simplification as for the energy centroid, disregarding local terms, which are later reintroduced through comparison with the hydrogenic limit. The entire calculation can then be conducted in $d = 3$ dimensions without requiring regularization.

The hyperfine mixing contribution is of the order α^6, and is given by the second-order expression with Fermi contact interaction operator

$$E^{(6)}_{\mathrm{mix}} = \frac{\left\langle 2^3S|V_F|2^1S\right\rangle^2}{E_0(2^3S) - E_0(2^1S)}\,. \tag{4.43}$$

Formally, it is of the second order in electron to nucleus mass ratio, and one would expect it to be small. However, due to small difference between energies of the 2^3S and 2^1S states it is greatly enhanced. In addition to Eq. (4.43) we have to include also the higher order corrections to it. At our level of precision they are significant and cannot be omitted [9]. Specifically, we need to include relativistic and recoil corrections to Eq. (4.43), along with the correction arising from the mixing with higher excited states.

The total theoretical result for 2^3S hfs of ^{3}He obtained by us is

$$\nu_{\mathrm{hfs}}(\mathrm{theo}) = -6\,739\,701\,181(41)\,\mathrm{Hz}\,, \tag{4.44}$$

where we improved the accuracy by a factor of 40 in comparison with previous calculations. We can compare it with the experimental value [10]

$$\nu_{\mathrm{hfs}}(\mathrm{exp}) = -6\,739\,701\,177(16)\,\mathrm{Hz}\,. \tag{4.45}$$

The agreement between theory and experiment is exceptional, and with an uncertainty of 41 Hz, it represents the most accurate theoretical result ever attained for non-hydrogenic systems.

The excellent agreement of theory and experiment for the helium hfs contrasts sharply with the 9σ discrepancy observed for the HD^+ [84]. The disagreement is very surprising because the same theoretical approach is used in both systems. If the discrepancy is confirmed in forthcoming studies, this would be a signal of some unknown physics.

4.3.1 Hyperfine structure of $^{6,7}Li^+$

The results of our hfs calculation can be extended to heliumlike ions, in particular to Li^+, for which accurate experimental data is available. In our paper [34] we calculated 2^3S state hfs of isotopes $^{6,7}Li^+$. Hyperfine splitting of Li^+ is given by a combination of the magnetic dipole and electric quadrupole hyperfine structure contributions,

$$E_{\rm hfs} = A\,\langle \vec{I}\cdot\vec{S}\rangle + B\,\langle (I^iI^j)^{(2)}(S^iS^j)^{(2)}\rangle\,, \tag{4.46}$$

where $\vec{S}=\vec{s}_1+\vec{s}_2$ is the total spin of electrons, and the symmetric traceless tensors in the quadrupole term are defined in the same way as the expression in Eq. (3.5). By appropriately combining experimental hfs transitions, one may eliminate the electric quadrupole part of Eq. (4.46) and extract the value for the coefficient A. For atomic Li, as well as for Li^{2+} and ^{3}He, the quadrupole contribution vanishes automatically. The remaining contribution to hfs will then again be in the form of series (4.41). By comparing theoretical results for pointlike nucleus with the measured hfs of Li^+, one can determine the nuclear structure contribution $\delta_{\rm nuc}$, parametrized in terms of the effective Zemach radius $\widetilde{r}_Z$.

For evaluation of hfs one needs to use accurate value of nuclear g-factor. The nuclear g-factor g_I of an atom is related to the free-nucleus g-factor g_N by the shielding constant σ,

$$g_I = g_N\,(1-\sigma)\,, \tag{4.47}$$

which can be calculated by the atomic theory. For a light atom, the shielding constant σ is effectively described by a double expansion in powers of the fine-structure constant α and the electron-to-nucleus mass ratio m/M,

$$\sigma = \alpha^2\,\sigma^{(2)} + \alpha^4\,\sigma^{(4)} + \alpha^2\,\frac{m}{M}\sigma^{(2,1)} + \dots\,. \tag{4.48}$$

In our work [85] we calculated the shielding constant and conducted a precise determination of the nuclear magnetic dipole moments of isotopes ^{6,7}Li from measured ratios of the nuclear and the electron g-factors. We notably improved the precision for the magnetic moments, and our results deviate significantly from those tabulated in Ref. [86]. The discrepancy arises because previous tabulations often overlooked uncertainties linked to theoretical calculations of diamagnetic corrections.

Utilizing our enhanced values for nuclear g-factors, we calculated $^{6,7}Li^+$ hfs for pointlike nucleus and used it for determination of the effective Zemach radii [34]. For ^{6}Li our results compared to the ones in the literature are

$$\widetilde{r}_Z(^6Li^+) = 2.39(2)\,{\rm fm}\,, \tag{4.49}$$
$$\widetilde{r}_Z(^6Li^+)[87] = 2.44\,(2)\,{\rm fm}\,, \tag{4.50}$$
$$\widetilde{r}_Z(^6Li^+)[88] = 2.40\,(16)\,{\rm fm}\,, \tag{4.51}$$
$$\widetilde{r}_Z(^6Li^+)[88] = 2.47\,(8)\,{\rm fm}\,, \tag{4.52}$$
$$\widetilde{r}_Z(^6Li)[89] = 2.29\,(4)\,{\rm fm}\,, \tag{4.53}$$

and for ^{7}Li they are

$$\widetilde{r}_Z(^7\mathrm{Li}^+) = 3.33(3)\,\mathrm{fm}\,, \tag{4.54}$$
$$\widetilde{r}_Z(^7\mathrm{Li}^+)[88] = 3.33\,(7)\,\mathrm{fm}\,, \tag{4.55}$$
$$\widetilde{r}_Z(^7\mathrm{Li}^+)[88] = 3.38\,(3)\,\mathrm{fm}\,, \tag{4.56}$$
$$\widetilde{r}_Z(^7\mathrm{Li})[89] = 3.23\,(4)\,\mathrm{fm}\,. \tag{4.57}$$

We confirmed the surprising result that the effective Zemach radius of ^{6}Li is smaller than for ^{7}Li, in spite of the fact that for the nuclear charge radius the situation is reversed. The probable explanation is a large contribution of inelastic effects. Additionally, we noted a 2σ deviation in the effective Zemach radius determined from Li^+ ion compared to that from Li atom [89]. This is likely caused by larger than expected α^7 contribution in Li atom, which was estimated based on hydrogenic results and not rigorously calculated. The contribution of the order α^6 calculated in [89] for Li atom already differs by approximately 50% from the hydrogenic value, indicating that a similar discrepancy might be present for the order α^7 as well.

In summary, this Chapter demonstrates that for heliumlike systems, it is possible to calculate energy levels with nearly the same accuracy as in hydrogen. Comparisons between measurements and theoretical predictions in helium can be employed for testing QED or determining fundamental constants. The potential for further improvement lies in identifying the source of the discrepancy between theory and experiment for ionization energies. Once this discrepancy is addressed, it becomes feasible to extend the calculation to singlet states and utilize the results to obtain the absolute value for the charge radius of helium.

5. Conclusions

To summarize the preceding Chapters, the author and his coworkers accomplished the following results in years 2014-2024:

- We investigated the energy levels of two-body systems with arbitrary constituent particles up to the order α^6 in NRQED theory. The derived formulas are applicable to both spinless and spin-1/2 particles, whether pointlike or hadronic, and for angular momentum $l \geq 1$. We checked that for specific limit cases the results are in accordance with Dirac and Klein-Gordon equation. Furthermore, our results can be extended to exotic atoms like muonic hydrogen, positronium, or protonium. These results were published in [35, 36]. In the case of muonic helium ion, we used our results to determine fine structure splitting of $2P$ states. Specifically, for $^3He^+$ this amounted to 144.785(3) meV, and for $^4He^+$ to 146.182(3) meV, in accordance with experimental values 144.763(114) meV and 146.047(96) meV, respectively. In the future, we plan to calculate the contribution of the order α^7, which is important for positronium atom and also will serve as a check of our calculations of the α^7 contribution in helium.

- We published a review paper on hydrogenlike systems [5], comprehensively presenting all individual contributions to the Lamb shift. One of these contributions was a higher-order α^6 nuclear structure correction that we derived for both ordinary (electronic) and muonic hydrogenlike atoms in Ref. [90]. This allowed us to enhance the precision in determining the Lamb shift in various hydrogenlike ions. For instance, for the $2S - 2P_{1/2}$ transition in hydrogen, the theoretical result, incorporating the refined nuclear structure contribution, is 1.057 834 12(23)(13)GHz. The first uncertainty (23) represented the theoretical uncertainty, while the second one (13) was induced by uncertainties of nuclear radius and mass. This result was in agreement with experimental result 1.057 847(9)GHz from [91].

- We studied hyperfine splitting in hydrogenlike atoms. The comparison of our accurate theoretical calculations with experimental measurements can be used either to test QED or to extract the information about the nuclear structure effects. In the case of $^3He^+$ ion, we used our results to extract the information about the nuclear structure in terms of the effective Zemach radius. Conversely, for $^{6,7}Li^{2+}$ we obtained theoretical prediction for hyperfine splitting, which is currently not known experimentally. These results were published in [34, 60].

- In the case of helium atom, we calculated the higher-order recoil correction of the order $\alpha^6\, m/M$ for both singlet and triplet states. This allowed us to obtain accurate theoretical prediction for $^3He - {}^4He$ isotope shift of various transitions. Through a comparison with experimental data, we extracted values for the nuclear charge radii difference of ^3He and ^4He from different measurements. We showed that the obtained values are in disagreement with each other, which calls for verification of these experiments. These results were published in [24, 30, 31].

- For helium D states, we calculated the energy levels for states with $n = 3 \dots 6$, improving their theoretical precision. These results are in 10σ discrepancy with previous calculations, due to the previously underestimated nonradiative α^6 contributions. Additionaly, we derived general formula for the nonrecoil α^6 contribution for arbitrary light atoms. We presented these results in papers [32, 70, 71].

- We derived a complete correction of the order α^7 to energy centroid for helium triplet states. This correction consisted of three parts: relativistic corrections to Bethe logarithm, radiative corrections, and nonradiative photon exchange corrections. We observed that for $2^3S - 2^3P$ transition the theoretical prediction of 276 736 495.620 (54)MHz was in excellent agreement with the measurement of 276 736 495.600 0 (14) MHz, while for the ionization energies of individual triplet states, we have up to 10σ discrepancy with experiment. The source of this discrepancy is not known at the present time. Later, we extended our calculation also to heliumlike ions, and our results were again in agreement with experiment for the $2^3S - 2^3P$ transition. The only exception was for Be^{2+} which, however, had already been reported to disagree with theory for the fine structure. Independent verification of this experiment is thus needed. These results were published in papers [7, 28, 29, 33, 66, 67, 77]. In the future, this calculation can be extended also to helium singlet states. For these states, the derivation is much more complicated but we believe it is still feasible.

- For heliumlike ions, we derived correction to the hyperfine splitting of the order α^7. In the case of 2^3S in ^{3}He, with the help of the nuclear structure contribution extracted from $^3He^+$ ion, we achieved a theoretical prediction of $-6\,739\,701\,181(41)$ Hz, in perfect agreement with the experimental result of $-6\,739\,701\,177(16)$ Hz. The discrepancy between theory and experiment is merely 4 Hz, with a theoretical uncertainty of 41 Hz, rendering it the most accurate theoretical prediction for nonhydrogenic systems to date. In the case of heliumlike isotopes $^{6,7}Li^+$, we utilized theoretical predictions to determine the effective Zemach radius, confirming that the value for ^{7}Li is approximately by 40% larger than that of ^{6}Li. For that we also calculated magnetic shielding in Li and used it to improve the value of lithium magnetic dipole moments. These results were presented in papers [9, 34, 85].

Many of the topics addressed in preceding Chapters represent ongoing projects with potential for further exploration. For example, addressing the discrepancy in the energy centroid ionization energies in helium is crucial for reliably extracting the nuclear charge radius. Several experimental groups are currently conducting measurements, underscoring the demand for accurate theoretical results. Another unresolved matter is the question of nuclear polarizability effects. As of now, we are unable to explicitly calculate their contribution. Therefore, we parameterize the nuclear structure effects in terms of the effective Zemach radius. Confirming the surprisingly large effective Zemach radius of ^{7}Li compared to the one of ^{6}Li, this calls for deeper investigation of the nuclear structure. Thus, there remain numerous opportunities for extending our research and delving further into these unresolved areas.

Bibliography

[1] S. Sturm et al., Nature (London) **506**, 467 (2014).

[2] K. Pachucki, U. D. Jentschura, and V. A. Yerokhin, Phys. Rev. Lett. **93**, 150401 (2004); **94**, 229902(E) (2005); K. Pachucki, A. Czarnecki, U. D. Jentschura, and V. A. Yerokhin, Phys. Rev. A **72**, 022108 (2005).

[3] U. D. Jentschura and V. A. Yerokhin, Phys. Rev. A **73**, 062503 (2006).

[4] R. G. Bullis, C. Rasor, W. L. Tavis, S. A. Johnson, M. R. Weiss, and D. C. Yost, Phys. Rev. Lett. **130**, 203001 (2023).

[5] V. A. Yerokhin, K. Pachucki, V. Patkóš, Ann. Phys. (Berl.) **531**, 1800324 (2018).

[6] A. Matveev et al., Phys. Rev. Lett. **110**, 230801 (2013).

[7] V. Patkóš, V. A. Yerokhin, K. Pachucki, Phys. Rev. A **103**, 042809 (2021).

[8] X. Zheng, Y. R. Sun, J.-J. Chen, W. Jiang, K. Pachucki, and S.-M. Hu, Phys. Rev. Lett. **119**, 263002 (2017).

[9] V. Patkóš, V. A. Yerokhin, K. Pachucki, Phys. Rev. Lett. **131**, 183001 (2023).

[10] S. D. Rosner and F. M. Pipkin, Phys. Rev. A **1**, 571 (1970); 3, 521(E) (1971).

[11] M. Kalinowski, K. Pachucki, and V. A. Yerokhin, Phys. Rev. A **98**, 062513 (2018).

[12] G. Clausen, P. Jansen, S. Scheidegger, J. A. Agner, H. Schmutz, and F. Merkt Phys. Rev. Lett. **127**, 093001 (2021).

[13] E. Tiesinga, P. J. Mohr, D. B. Newell, and B. N. Taylor Rev. Mod. Phys. **93**, 025010 (2021).

[14] M. I. Eides, H. Grotch, and V. A. Shelyuto, Phys. Rep. **342**, 63 (2001).

[15] J. B. French and V. F. Weisskopf, Phys. Rev. **75**, 1240 (1949); N. M. Kroll and W. E. Lamb, Phys. Rev. **75**, 388 (1949).

[16] V. M. Shabaev, Theor. Math. Phys. **63**, 588 (1985). See also V. M. Shabaev, Sov. J. Nucl. Phys. **47**, 69 (1988).

[17] H. A. Bethe, Phys. Rev. **72**, 339 (1947).

[18] U. D. Jentschura, P. J. Mohr and G. Soff, Phys. Rev. A **63**, 042512 (2001).

[19] J. Zamastil, V. Patkóš, Phys. Rev. A **88**, 032501 (2013).

[20] J. Schwinger, Phys. Rev. **82**, 664 (1951).

[21] W. E. Caswell and G. P. Lepage, Phys. Lett. B **167**, 437 (1986).

[22] K. Pachucki, Phys. Rev. A **71**, 012503 (2005).

[23] K. Pachucki, Phys. Rev. A **74**, 022512 (2006).

[24] K. Pachucki, V. Patkóš, V. A. Yerokhin, Phys. Rev. A **95**, 062510 (2017).

[25] K. Pachucki, Phys. Rev. A **56**, 297 (1997).

[26] K. Pachucki, Phys. Rev. Lett. **79**, 4120 (1997); K. Pachucki and S. Karshenboim, *ibid.* **80**, 2101 (1998).

[27] A. Czarnecki, K. Melnikov, and A. Yelkhovsky, Phys. Rev. Lett. **82**, 311 (1999); Phys. Rev. A **59**, 4316 (1999).

[28] V. Patkóš, V. A. Yerokhin, and K. Pachucki, Phys. Rev. A **101**, 062516 (2020).

[29] V. Patkóš, V. A. Yerokhin, and K. Pachucki, Phys. Rev. A **103**, 012803 (2021).

[30] V. Patkóš, V. A. Yerokhin, and K. Pachucki, Phys. Rev. A **94**, 052508 (2016).

[31] V. Patkóš, V. A. Yerokhin, and K. Pachucki, Phys. Rev. A **95**, 012508 (2017).

[32] V. Patkóš, V. A. Yerokhin, K. Pachucki, Phys. Rev. A **100**, 042510 (2019).

[33] V. A. Yerokhin, V. Patkóš, and K. Pachucki, Phys. Rev. A **98**, 032503 (2018).

[34] K. Pachucki, V. Patkóš, and V. A. Yerokhin, Phys. Rev. A **108**, 052802 (2023).

[35] J. Zatorski, V. Patkóš, and K. Pachucki, Phys. Rev. A **106**, 042804 (2022).

[36] V. Patkóš, V. A. Yerokhin, and K. Pachucki, Phys. Rev. **109**, 022819 (2024).

[37] R. Pohl et al., Nature **466**, 213 (2010).

[38] A. Antognini et al., Science **339**, 417 (2013).

[39] H. Gao and M. Vanderhaeghen, Rev. Mod. Phys. **94**, 015002 (2022).

[40] A. Grinin et al., Science **370**, 1061–1066 (2020).

[41] A. Beyer et al., Science **358**, 79–85 (2017).

[42] H. A. Bethe and E. E. Salpeter, *Quantum Mechanics Of One-And Two-Electron Atoms* (Plenum, New York, 1977).

[43] H. Grotch and D. R. Yennie, Z. Phys **202**, 425 (1967); Rev. Mod. Phys. **41**, 350 (1969).

[44] E. E. Salpeter, Phys. Rev. 87, 328 (1952).

[45] G. S. Adkins, J. Gomprecht, Y. Li, and E. Shinn, Phys. Rev. Lett. **130**, 023004 (2023).

[46] Eberhard Widmann, Few-Body Systems **45**, 165 (2009).

[47] R. S. Hayano, M. Hori, D. Horvath and E. Widmann, Rep. Prog. Phys. **70**, 1995 (2007).

[48] M. Hori *et al.*, Phys. Rev. Lett. **94**, 063401 (2005).

[49] G. S. Adkins, B. Akers, M. F. Alam, L. M. Tram, and X. Zhang, Proc. Sci. **353**, 004 (2019).

[50] S. G. Karshenboim, E. Yu. Korzinin, V. A. Shelyuto, and V. G. Ivanov, Phys. Rev. A **96**, 022505 (2017).

[51] E. Yu. Korzinin, V. A. Shelyuto, V. G. Ivanov, and S. G. Karshenboim, Phys. Rev. A **97**, 012514 (2018).

[52] K. Schuhmann, L. M. P. Fernandes, F. Nez, M. A. Ahmed, F. D. Amaro, P. Amaro, F. Biraben, T.-L. Chen, D. S. Covita, A. J. Dax et al., arXiv:2305.11679.

[53] R. Pohl, F. Nez, L. M. P. Fernandes, F. D. Amaro, F. Biraben, J. M. R. Cardoso, D. S. Covita, A. Dax, S. Dhawan, M. Diepold et al., Science **353**, 669 (2016).

[54] L. Essen, R. Donaldson, E. Hope, and M. Bangham, Metrologia **9**, 128 (1973).

[55] S. G. Karshenboim, Phys. Rep. **422**, 1 (2005).

[56] S. G. Karshenboim, Phys. Rev. A **83**, 062119 (2011).

[57] A. C. Zemach, Phys. Rev. **104**, 1771 (1956).

[58] R. Pohl, F. Nez, L. M. P. Fernandes, F. D. Amaro, F. Biraben, J. M. R. Cardoso, D. S. Covita, A. Dax, S. Dhawan, M. Diepold *et al.*, Science **353**, 669 (2016).

[59] O. Tomalak, Phys. Rev. D **99**, 056018 (2019).

[60] V. Patkóš, V. A. Yerokhin, K. Pachucki, Phys. Rev. A **107**, 052802 (2023).

[61] I. Sick, Phys. Rev. C **90**, 064002 (2014).

[62] A. Schneider *et al.*, Nature (London) **606**, 878 (2022).

[63] V. I. Korobov, Phys. Rev. A **61**, 064503 (2000).

[64] F. Ficek, D. F. Jackson Kimball, M. G. Kozlov, N. Leefer, S. Pustelny, and D. Budker, Phys. Rev. A **95**, 032505 (2017).

[65] J. J. Krauth *et al.*, Nature (London) **589**, 527 (2021).

[66] V. A. Yerokhin, V. Patkóš, and K. Pachucki, Phys. Rev. A **106**, 022815 (2022).

[67] V. A. Yerokhin, V. Patkóš, and K. Pachucki, Phys. Rev. A **107**, 012810 (2023).

[68] K. Pachucki, J. Phys. B **31**, 5123 (1998).

[69] K. Pachucki, Phys. Rev. A **74**, 062510 (2006).

[70] A. Wienczek, K. Pachucki, M. Puchalski, V. Patkóš, V. A. Yerokhin, Phys. Rev. A **99**, 052505 (2019)

[71] V. A. Yerokhin, M. Puchalski, V. Patkóš, K. Pachucki, Phys. Rev. A **102**, 012807 (2020).

[72] D. C. Morton, Q. Wu, and G. W. F. Drake, Can. J. Phys. **84**, 83 (2006).

[73] V. A. Yerokhin, V. Patkóš, K. Pachucki, Symmetry **13**, 1246 (2021).

[74] R. van Rooij, J. S. Borbely, J. Simonet, M. D. Hoogerland, K. S. E. Eikema, R. A. Rozendaal, and W. Vassen, Science **333**, 196 (2011).

[75] P. C. Pastor, G. Giusfredi, P. De Natale, G. Hagel, C. de Mauro, and M. Inguscio, Phys. Rev. Lett. **92**, 023001 (2004); (E) *ibid.* **97**, 139903 (2006); P. Cancio Pastor, L. Consolino, G. Giusfredi, P. D. Natale, M. Inguscio, V. A. Yerokhin, and K. Pachucki, Phys. Rev. Lett. **108**, 143001 (2012).

[76] D. Shiner, R. Dixon, and V. Vedantham, Phys. Rev. Lett. **74**, 3553 (1995).

[77] V. A. Yerokhin, V. Patkóš, K. Pachucki, Eur. Phys. J. D **76**, 142 (2022).

[78] C. Dorrer, F. Nez, B. de Beauvoir, L. Julien, and F. Biraben, Phys. Rev. Lett. **78**, 3658 (1997).

[79] P.-L. Luo, J.-L. Peng, J. Hu, Y. Feng, L.-B. Wang, and J.-T. Shy, Phys. Rev. A **94**, 062507 (2016).

[80] T. J. Scholl, R. Cameron, S. D. Rosner, L. Zhang, R. A. Holt, C. J. Sansonetti, and J. D. Gillaspy, Phys. Rev. Lett. **71**, 2188 (1993).

[81] G. W. F. Drake, Can. J. Phys. **66**, 586 (1988). See also V. A. Yerokhin and K. Pachucki, Phys. Rev. A **81**, 022507 (2010).

[82] P. Imgram et al., Phys. Rev. Lett. **131**, 243001 (2024).

[83] K. Pachucki, J. Phys. B **34**, 3357 (2001); K. Pachucki, V. A. Yerokhin, and P. Cancio Pastor, Phys. Rev. A **85**, 042517 (2012).

[84] S. Patra et al., Science **369**, 1238 (2020); M. Haidar, V. I. Korobov, L. Hilico, and J.-P. Karr, Phys. Rev. A **106**, 042815 (2022).

[85] K. Pachucki, V. Patkóš, V. A. Yerokhin, Phys. Lett. B **846**, 138189 (2023)

[86] N.J. Stone, At. Data Nucl. Data Tables **90**, 75 (2005).

[87] W. Sun et al., Phys. Rev. Lett. **131**, 103002 (2023).

[88] X.-Q. Qi, P.-P. Zhang, Z.-C. Yan, G. W. F. Drake, Z.-X. Zhong, T.-Y. Shi, S.-L. Chen, Y. Huang, H. Guan, and K.-L. Gao, Phys. Rev. Lett. **125**, 183002 (2020).

[89] M. Puchalski and K. Pachucki, Phys. Rev. Lett. **111**, 243001 (2013).

[90] K. Pachucki, V. Patkóš, V. A. Yerokhin, Phys. Rev. A **97**, 062511 (2018).

[91] S. R. Lundeen, F. M. Pipkin, Metrologia **22**, 9 (1986).

A. List of publications

The following list summarizes the relevant publications in journals with impact factor where I am author or co-author.

- V. Patkóš, V. A. Yerokhin, K. Pachucki: "Two-body P-state energies at order α^6", Phys. Rev. A **109**, 022819 (2024). 10.1103/PhysRevA.109.022819
- K. Pachucki, V. Patkóš, V. A. Yerokhin: "Hyperfine splitting in $^{6,7}Li^+$", Phys. Rev. A **108**, 052802 (2023). doi:10.1103/PhysRevA.108.052802
- V. Patkóš, V. A. Yerokhin, K. Pachucki: "Higher-order QED corrections to hyperfine splitting in ^{3}He", Phys. Rev. Lett. **131**, 183001 (2023). doi:10.1103/PhysRevLett.131.183001
- K. Pachucki, V. Patkóš, V. A. Yerokhin: "Accurate determination of ^{6,7}Li nuclear magnetic moments", Phys. Lett. B **846**, 138189 (2023). doi:10.1016/j.physletb.2023.138189
- V. Patkóš, V. A. Yerokhin, K. Pachucki: "Nuclear polarizability effects in $^3He^+$ hyperfine splitting", Phys. Rev. A **107**, 052802 (2023). doi:10.1103/PhysRevA.107.052802
- V. A. Yerokhin, V. Patkóš, K. Pachucki: "QED $m\alpha^7$ effects for triplet states of heliumlike ions", Phys. Rev. A **107**, 012810 (2023). doi:10.1103/PhysRevA.107.012810
- J. Zatorski, V. Patkóš, K. Pachucki: "Quantum electrodynamics of two-body systems with arbitrary masses up to α^6 order", Phys. Rev. A **106**, 042804 (2022). doi:10.1103/PhysRevA.106.042804
- V. A. Yerokhin, V. Patkóš, K. Pachucki: "QED calculations of energy levels of heliumlike ions with $5 \leq Z \leq 30$", Phys. Rev. A **106**, 022815 (2022). doi:10.1103/PhysRevA.106.022815
- V. A. Yerokhin, V. Patkóš, K. Pachucki: "Relativistic Bethe logarithm for triplet states of helium-like ions", Eur. Phys. J. D **76**, 142 (2022). doi:10.1140/epjd/s10053-022-00474-8
- V. A. Yerokhin, V. Patkóš, K. Pachucki: "Atomic structure calculations of helium with correlated exponential functions", Symmetry **13**, 1246 (2021). doi:10.3390/Sym13071246
- V. Patkóš, V. A. Yerokhin, K. Pachucki: "Complete $\alpha^7 m$ Lamb shift of helium triplet states", Phys. Rev. A **103**, 042809 (2021). doi:10.1103/PhysRevA.103.042809

- V. Patkóš, V. A. Yerokhin, K. Pachucki: "Radiative $\alpha^7 m$ contribution to the helium Lamb shift", Phys. Rev. A **103**, 012803 (2021). doi:10.1103/PhysRevA.103.012803
- V. A. Yerokhin, M. Puchalski, V. Patkóš, K. Pachucki: "QED calculation of ionization energies of 1snd states in helium", Phys. Rev. A **102**, 012807 (2020). doi:10.1103/PhysRevA.102.012807
- V. Patkóš, V. A. Yerokhin, K. Pachucki: "Nonradiative $\alpha^7 m$ QED effects in the Lamb shift of helium triplet states", Phys. Rev. A **101**, 062516 (2020). doi:10.1103/PhysRevA.101.062516
- V. Patkóš, V. A. Yerokhin, K. Pachucki: "Complete quantum electrodynamic $\alpha^6 m$ correction to energy levels of light atoms", Phys. Rev. A **100**, 042510 (2019). doi:10.1103/PhysRevA.100.042510
- A. Wienczek, K. Pachucki, M. Puchalski, V. Patkóš, V. A. Yerokhin: "Quantum electrodynamic corrections to the 1s3d states of the helium atom", Phys. Rev. A **99**, 052505 (2019). doi:10.1103/PhysRevA.99.052505
- V. A. Yerokhin, K. Pachucki, V. Patkóš: "Theory of the Lamb Shift in Hydrogen and Light Hydrogen-Like Ions", Ann. Phys. (Berl.) **531**, 1800324 (2018). doi:10.1002/andp.201800324
- V. A. Yerokhin, V. Patkóš, K. Pachucki: "Relativistic corrections to the Bethe logarithm for the 2^3S and 2^3P states of He", Phys. Rev. A **98**, 032503 (2018). doi:10.1103/PhysRevA.98.032503
- K. Pachucki, V. Patkóš, V. A. Yerokhin: "Three-photon-exchange nuclear structure correction in hydrogenic systems", Phys. Rev. A **97**, 062511 (2018). doi:10.1103/PhysRevA.97.062511
- K. Pachucki, V. Patkóš, V. A. Yerokhin: "Testing fundamental interactions on the helium atom", Phys. Rev. A **95**, 062510 (2017). doi:10.1103/PhysRevA.95.062510
- V. Patkóš, V. A. Yerokhin, K. Pachucki: "Higher-order recoil corrections for singlet states of the helium atom", Phys. Rev. A **95**, 012508 (2017). doi:10.1103/PhysRevA.95.012508
- V. Patkóš, J. Zamastil, D. Šimsa: "Nonrelativistic QED expansion for the electron self-energy", Phys. Rev. A **95**, 012507 (2017). doi:10.1103/PhysRevA.95.012507
- V. Patkóš, V. A. Yerokhin, K. Pachucki: "Higher-order recoil corrections for triplet states of the helium atom", Phys. Rev. A **94**, 052508 (2016). doi:10.1103/PhysRevA.94.052508

- V. Patkóš, J. Zamastil: "Lamb shift for states with $j = 1/2$", Phys. Rev. A **91**, 062511 (2015).
  doi:10.1103/PhysRevA.86.042514

- J. Zamastil, V. Patkóš: "Self-energy of an electron bound in a Coulomb field", Phys. Rev. A **88**, 032501 (2013).
  doi:10.1103/PhysRevA.88.032501

- J. Zamastil, V. Patkóš: "Self-energy of a bound electron for excited states", Phys. Rev. A **86**, 042514 (2012).
  doi:10.1103/PhysRevA.86.042514